Journal of Visualized Experiments

Microfluidic Fabrication Techniques for High-Pressure Testing of Microscale Supercritical CO2 Foam Transport in Fractured Unconventional Reservoirs

--Manuscript Draft--

Article Type:	Invited Methods Article - JoVE Produced Video
Manuscript Number:	JoVE61369R2
Full Title:	Microfluidic Fabrication Techniques for High-Pressure Testing of Microscale Supercritical CO2 Foam Transport in Fractured Unconventional Reservoirs
Section/Category:	JoVE Engineering
Keywords:	scCO2 Foam; Fractured Reservoirs; Unconventional Reservoirs; Shale, Microfluidics; Photolithography; Wet Etching; Thermal Bonding; Selective Laser-induced Etching
Corresponding Author:	Saman A. Aryana University of Wyoming Laramie, WY UNITED STATES
Corresponding Author's Institution:	University of Wyoming
Corresponding Author E-Mail:	saryana@uwyo.edu
Order of Authors:	Hooman Hosseini
	Feng Guo
	Reza Barati Ghahfarokhi
	Saman A. Aryana
Additional Information:	
Question	**Response**
Please indicate whether this article will be Standard Access or Open Access.	Standard Access (US$2,400)
Please indicate the **city, state/province, and country** where this article will be **filmed**. Please do not use abbreviations.	Laramie, WY, USA

TITLE:

Microfluidic Fabrication Techniques for High-Pressure Testing of Microscale Supercritical CO_2 Foam Transport in Fractured Unconventional Reservoirs

AUTHORS AND AFFILIATIONS:

Hooman Hosseini[1], Feng Guo[2], Reza Barati Ghahfarokhi[1], Saman A. Aryana[2]

[1]Department of Chemical and Petroleum Engineering, University of Kansas, Lawrence, Kansas 66045, USA

[2]Department of Chemical Engineering, University of Wyoming, Laramie, WY 82071, USA

Email addresses of co-authors:

Hooman Hosseini (h.hosseini@ku.edu)

Feng Guo (fguo@uwyo.edu)

Corresponding authors:

Saman A. Aryana (saryana@uwyo.edu)

Reza Barati Ghahfarokhi (reza.barati@ku.edu)

KEYWORDS:

$scCO_2$ Foam, Fractured Reservoirs, Unconventional Reservoirs, Shale, Microfluidics, Photolithography, Wet Etching, Thermal Bonding, Selective Laser-induced Etching

SUMMARY:

This paper describes a protocol along with a comparative study of two microfluidic fabrication techniques, namely photolithography/wet-etching/thermal-bonding and Selective Laser-induced Etching (SLE), that are suitable for high-pressure conditions. These techniques constitute enabling platforms for direct observation of fluid flow in surrogate permeable media and fractured systems under reservoir conditions.

ABSTRACT:

Pressure limitations of many microfluidic platforms have been a significant challenge in microfluidic experimental studies of fractured media. As a result, these platforms have not been fully exploited for direct observation of high-pressure transport in fractures. This work introduces microfluidic platforms that enable direct observation of multiphase flow in devices featuring surrogate permeable media and fractured systems. Such platforms provide a pathway to address important and timely questions such as those related to CO_2 capture, utilization and storage. This work provides a detailed description of the fabrication techniques and an experimental setup that may serve to analyze the behavior of supercritical CO_2 ($scCO_2$) foam, its structure and stability. Such studies provide important insights regarding enhanced oil recovery processes and the role of hydraulic fractures in resource recovery from unconventional reservoirs. This work presents a comparative study of microfluidic devices developed using two different techniques: photolithography/wet-etching/thermal-bonding versus Selective Laser-induced Etching. Both techniques result in devices that are chemically and physically resistant and tolerant of high

pressure and temperature conditions that correspond to subsurface systems of interest. Both techniques provide pathways to high-precision etched microchannels and capable lab-on-chip devices. Photolithography/wet-etching, however, enables fabrication of complex channel networks with complex geometries, which would be a challenging task for laser etching techniques. This work summarizes a step-by-step photolithography, wet-etching and glass thermal-bonding protocol and, presents representative observations of foam transport with relevance to oil recovery from unconventional tight and shale formations. Finally, this work describes the use of a high-resolution monochromatic sensor to observe $scCO_2$ foam behavior where the entirety of the permeable medium is observed simultaneously while preserving the resolution needed to resolve features as small as 10 µm.

INTRODUCTION:

Hydraulic fracturing has been used for quite some time as a means to stimulate flow especially in tight formations[1]. Large amounts of water needed in hydraulic fracturing are compounded with environmental factors, water-availability issues[2], formation damage[3], cost[4] and seismic effects[5]. As a result, interest in alternate fracturing methods such as waterless fracturing and the use of foams is on the rise. Alternative methods may provide important benefits such as reduction in water use[6], compatibility with water sensitive formations[7], minimal to no plugging of the formation[8], high apparent viscosity of the fracturing fluids[9], recyclability[10], ease of clean-up and proppant carrying capability[6]. CO_2 foam is a potential waterless fracturing fluid that contributes to more efficient production of petroleum fluids and improved CO_2 storage capacities in the subsurface with a potentially smaller environmental footprint compared to conventional fracturing techniques[6,7,11].

Under optimal conditions, supercritical CO_2 foam ($scCO_2$ foam) at pressures beyond the minimum miscibility pressure (MMP) of a given reservoir provides a multi-contact miscible system that is able to direct flow into less permeable parts of the formation, thereby improving sweep efficiency and recovery of the resources[12,13]. $scCO_2$ delivers gas like diffusivity and liquid like density[14] and is well suited for subsurface applications, such as oil recovery and carbon capture, utilization and storage (CCUS)[13]. The presence of the constituents of foam in the subsurface helps reduce the risk of leakage in long-term storage of CO_2[15]. Moreover, coupled-compressibility-thermal shock effects of $scCO_2$ foam systems may serve as effective fracturing systems[11]. Properties of CO_2 foam systems for subsurface applications have been studied extensively at various scales, such as characterization of its stability and viscosity in sand-pack systems and its effectiveness in displacement processes[3,6,12,15–17]. Fracture level foam dynamics and its interactions with porous media are less studied aspects that are directly relevant to the use of foam in tight and fractured formations.

Microfluidic platforms enable direct visualization and quantification of the relevant microscale processes. These platforms provide real-time control of the hydrodynamics and chemical reactions to study pore-scale phenomena alongside recovery considerations[1]. Foam generation, propagation, transport and dynamics may be visualized in microfluidic devices emulating fractured systems and fracture-microcrack-matrix conductive pathways relevant to oil recovery from tight formations. Fluid exchange between fracture and matrix is directly expressed in

accordance with the geometry[18], thereby highlighting the importance of simplistic and realistic representations. A number of relevant microfluidic platforms have been developed over the years to study various processes. For example, Tigglaar and coworkers discuss fabrication and high-pressure testing of glass microreactor devices through in-plane connection of fibers to test flow through glass capillaries connected to the microreactors[19]. They present their findings related to bond inspection, pressure tests and in-situ reaction monitoring by ^{1}H NMR spectroscopy. As such, their platform may not be optimal for relatively large injection rates, pre-generation of multiphase fluid systems for in situ visualization of complex fluids in permeable media. Marre and coworkers discuss the use of a glass microreactor to investigate high-pressure chemistry and supercritical fluid processes[20]. They include results as a finite-element simulation of stress distribution to explore the mechanical behavior of modular devices under the load. They use nonpermanent modular connections for interchangeable microreactor fabrication, and the silicon/Pyrex microfluidic devices are not transparent; these devices are suited for kinematic study, synthesis and production in chemical reaction engineering where visualization is not a primary concern. The lack of transparency makes this platform unsuitable for direct, in situ visualization of complex fluids in surrogate media. Paydar and coworkers present a novel way to prototype modular microfluidics using 3D printing[21]. This approach does not seem well-suited for high-pressure applications since it uses a photocurable polymer and the devices are able to withstand only up to 0.4 MPa. Most microfluidic experimental studies related to transport in fractured systems reported in literature focus on ambient temperature and relatively low-pressure conditions[1]. There have been several studies with a focus on direct observation of microfluidic systems that mimic subsurface conditions. For example, Jimenez-Martinez and co-workers introduce two studies on critical pore-scale flow and transport mechanisms in a complex network of fractures and matrix[22,23]. The authors study three-phase systems using microfluidics under reservoir conditions (8.3 MPa and 45 °C) for production efficiency; they assess $scCO_2$ usage for re-stimulation where the leftover brine from a prior fracturing is immiscible with CO_2 and the residual hydrocarbon[23]. Oil-wet silicon microfluidic devices have relevance to mixing of oil-brine-$scCO_2$ in Enhanced Oil Recovery (EOR) applications; however, this work does not directly address pore-scale dynamics in fractures. Another example is work by Rognmo et al. who study an upscaling approach for high-pressure, in situ CO_2 foam generation[24]. Most of the reports in literature that leverage microfabrication are concerned with CO_2-EOR and they often do not include important fabrication details. To the best of the authors' knowledge, a systematic protocol for fabrication of high-pressure capable devices for fractured formations is currently missing from the literature.

This work presents a microfluidic platform that enables the study of $scCO_2$ foam structures, bubble shapes, sizes and distribution, lamella stability in the presence of oil for EOR and hydraulic fracturing and aquifer remediation applications. The design and fabrication of microfluidic devices using optical lithography and Selective Laser-induced Etching[29] (SLE) are discussed. Additionally, this work describes fracture patterns that are intended to simulate the transport of fluids in fractured tight formations. Simulated pathways may range from simplified patterns to complex microcracks based on tomography data or other methods that provide information regarding realistic fracture geometries. The protocol describes step-by-step fabrication instructions for glass microfluidic devices using photolithography, wet-etching and thermal

bonding. An in-house developed collimated Ultra-Violet (UV) light source is used to transfer the desired geometric patterns onto a thin layer of photoresist, which is ultimately transferred to the glass substrate using a wet-etching process. As part of quality assurance, the etched patterns are characterized using confocal microscopy. As an alternative to photolithography/wet-etching, an SLE technique is employed to create a microfluidic device and a comparative analysis of the platforms is presented. The setup for flow experiments comprise gas cylinders and pumps, pressure controllers and transducers, fluid mixers and accumulators, microfluidic devices, high-pressure capable stainless-steel holders along with a high-resolution camera and an illumination system. Finally, representative samples of observations from flow experiments are presented.

PROTOCOL:

CAUTION: This protocol involves handling a high-pressure setup, a high-temperature furnace, hazardous chemicals, and UV light. Please read all relevant material safety data sheets carefully and follow chemical safety guidelines. Review pressure testing (hydrostatic and pneumatic) safety guidelines including required training, safe operation of all equipment, associated hazards, emergency contacts, etc. before starting the injection process.

1. Design geometrical patterns

1.1. Design a photomask comprising geometrical features and flow pathways of interest (**Figure 1**, **Supplementary File 1: Figure S1**).

1.2. Define the bounding box (surface area of the device) to identify the area of the substrate and confine the design to the dimensions of the desired medium.

1.3. Design inlet/outlet ports. Choose port dimensions (e.g., 4 mm in diameter in this case) to achieve a relatively uniform distribution of foam prior to entering the medium (**Figure 1**).

1.4. Prepare a photomask of the designed geometrical pattern by printing the design onto a sheet of transparent film or a glass substrate.

1.4.1. Extrude the two-dimensional design to the third dimension and incorporate inlet and outlet ports (for use in SLE).

NOTE: The SLE technique requires a three-dimensional drawing (**Figure 2**).

2. Transfer the geometric patterns to the glass substrate using photolithography

NOTE: Etchants and piranha solutions must be handled with extreme care. Use of personal protective equipment including facepiece reusable respirator, goggles, gloves and use of acid/corrosion resistant tweezers (**Table of Materials**) is recommended.

2.1. Prepare the solutions needed in the wet-etching process by following these steps (also see the electronic supporting information provided as **Supplementary File 1**).

2.1.1. Pour an adequate amount of chrome etchant solution in a beaker such that the substrate can be submerged in the etchant. Heat up the fluid to approximately 40 °C.

2.1.2. Prepare a solution of developer (**Table of Materials**) in deionized water (DI water) with a volumetric ratio of 1:8 such that the substrate is able to be fully submerge in the mixture.

2.2. Imprint the geometrical pattern on a borosilicate substrate coated with a layer of chromium and a layer of photoresist using UV irradiation.

2.2.1. Using gloved hands, place the mask (glass substrate or the transparent film bearing the geometrical pattern) directly on the side of the borosilicate substrate that is covered with chrome and photoresist.

2.2.2. Place the photomask and substrate combination under the UV light with the photomask facing the source.

NOTE: This work uses UV light with a wavelength of 365 nm (to match the peak sensitivity of the photoresist) and at an average intensity of 4.95 mW/cm^2.

2.2.3. Transfer the geometrical pattern into the layer of photoresist by exposing the stack of the substrate and the mask to UV light.

NOTE: Optimum exposure time is a function of the thickness of the photoresist layer and the strength of UV radiation. Photoresist is sensitive to light and the entire process of imprinting the pattern must be performed in a dark room equipped with yellow lighting.

2.3. Develop the photoresist.

2.3.1. Remove the photomask and substrate stack from the UV stage using gloved hands.

2.3.2. Remove the photomask and submerge the substrate in the developer solution for approximately 40 s, thereby transferring the pattern to the photoresist.

2.3.3. Cascade-rinse the substrate by flowing DI water from the top of the substrate and over all its surfaces a minimum of three times and allow the substrate to dry.

2.4. Etch the pattern in the chrome layer.

2.4.1. Submerge the substrate in a chrome etchant heated to about 40 °C for approximately 40 s, thereby transferring the pattern from the photoresist to the chrome layer.

2.4.2. Remove the substrate from the solution, cascade-rinse the substrate using DI water and allow it to dry.

2.5. Etch the pattern in the borosilicate substrate.

NOTE: A buffered etchant (**Table of Materials**) is used to transfer the geometrical pattern to the glass substrate. Prior to the use of the buffered etchant, the backside of the substrate is coated with a layer of photoresist to shield it from the etchant. The thickness of this protective layer is immaterial to the overall fabrication process.

2.5.1. Using a brush, apply several layers of hexamethyldisilazane (HMDS) on the uncovered face of the substrate and allow it to dry.

NOTE: HMDS helps promote adhesion of photoresist to the surface of the borosilicate substrate.

2.5.2. Apply one layer of photoresist on top of the primer. Place the substrate in an oven at 60–90 °C for 30–40 min.

2.5.3. Pour an adequate amount of the etchant into a plastic container and fully submerge the substrate in the etchant.

NOTE: The etching rate is influenced by the concentration, temperature and duration of exposure. The buffered etchant used in this work etches an average of 1–10 nm/min.

2.5.4. Leave the patterned substrate in the etchant solution for a predetermined amount of time based on the desired channel depths.

NOTE: Etching time may be reduced by intermittent bath sonication of the solution.

2.5.5. Remove the substrate from the etchant using a solvent-resistant pair of tweezers and cascade-rinse the substrate using DI water.

2.5.6. Characterize the etched features on the substrate to ensure desired depths have been achieved.

NOTE: This characterization may be done using a laser scanning confocal microscope (**Figure 3**). In this work, a 10x magnification is used for data acquisition. Once channel depths are satisfactory, move to the cleaning and bonding stage.

3. Clean and bond

3.1. Remove photoresist and chrome layers.

3.1.1. Remove the photoresist from the substrate by exposing the substrate to an organic solvent, such as N-Methyl-2-pyrrolidone (NMP) solution heated using a hot plate under a hood to approximately 65 °C for approximately 30 min.

3.1.2. Cascade-rinse the substrate with acetone (ACS grade), followed by ethanol (ACS grade) and DI water.

3.1.3. Place the cleaned substrate in chrome etchant heated using a hot plate under a hood to approximately 40 °C for about 1 min, thus removing the chrome layer from the substrate.

3.1.4. Once the substrate is free from chrome and photoresist, characterize the channel depths using laser scanning confocal microscopy.

NOTE: This work uses a 10x magnification for data acquisition (**Figure 4**).

3.2. Prepare the cover plate and the etched substrate for bonding.

3.2.1. Mark the positions of the inlet/out holes on a blank borosilicate substrate (cover plate) by aligning the cover plate against the etched substrate.

3.2.2. Blast through-holes in the marked locations using a micro abrasive sandblaster and 50 µm aluminum-oxide micro sandblasting media.

NOTE: Alternatively, the ports may be created using a mechanical drill.

3.2.3. Cascade rinse both the etched substrate and the cover plate with DI water.

3.2.4. Perform an RCA wafer cleaning procedure to remove contaminants prior to bonding using standard technique. Perform the wafer cleaning steps under a hood due to the volatility of the solutions involved in the process.

3.2.5. Bring a 1:4 by volume H_2O_2:H_2SO_4 piranha solution to a boil and submerge the substrate and the cover plate in the solution for 10 min under a hood.

3.2.6. Cascade rinse the substrate and the cover plate with DI water.

3.2.7. Submerge the substrate and the cover plate in the buffered etchant for 30–40 s.

3.2.8. Cascade rinse the substrate and the cover plate with DI water.

3.2.9. Submerge the substrate and the cover plate for 10 min in a 6:1:1 by volume DI water:H_2O_2:HCl solution that is heated to approximately 75 °C.

NOTE: Etching and bonding are preferably performed in a cleanroom. If a cleanroom is not available, performing the following steps in a dust-free environment is recommended. In this work, steps 3.2.9–3.2.12 are performed in a glovebox to minimize the possibility of contamination of the substrates.

3.2.10. Press the substrate and the cover plate tightly against each other while submerged.

3.2.11. Remove the substrate and the cover plate from DI water:H_2O_2:HCl solution. Cascade rinse with DI water and submerge in DI water.

3.2.12. Make sure the substrate and the cover plate are firmly attached together and carefully remove the two while pressed against each other from DI water.

3.3. Bond the substrates thermally.

3.3.1. Place the stacked substrates (the etched substrate and the cover plate) between two smooth, 1.52 cm-thick, glass-ceramic plates for bonding.

3.3.2. Place the glass-ceramic plates between two metallic plates made of Alloy X (**Table of Materials**), which is able to withstand the required temperatures without significant distortion.

3.3.3. Center the glass wafers in the ceramic-metallic holder.

NOTE: This work uses glass-ceramic plates that are 10 cm x 10 cm x 1.52 cm in thickness. The stacked setup is secured using 1/4" bolts and nuts (**Figure 5**).

3.3.4. Hand-tighten the nuts and place the holder in a vacuum chamber for 60 min at approximately 100 °C.

3.3.5. Remove the holder from the chamber and carefully tighten the nuts using approximately 10 lb-in of torque.

3.3.6. Place the holder inside a furnace and execute the following heating program. Raise the temperature at 1 °C/min up to 660 °C; keep the temperature constant at 660 °C for 6 h followed by a cooling step at approximately 1 °C/min back down to room temperature.

3.3.7. Remove the thermally bonded microfluidic device, rinse it with DI water, place it in HCl (12.1 M) and bath-sonicate (40 kHz at 100 W of power) the solution for one hour (**Figure 6**).

4. Fabricate laser-etched glass microfluidic devices

NOTE: Device fabrication was performed by a third-party glass 3D printing service (**Table of Materials**) via an SLE process and using a fused silica substrate as the precursor.

4.1. Write the desired pattern in a fused silica substrate using a linearly polarized laser beam oriented perpendicular to the stage generated via a femtosecond laser source with a pulse duration of 0.5 ns, a repetition rate of 50 kHz, pulse energy of 400 nJ, and a wavelength of 1.06 µm.

4.2. Remove the glass from the written pattern inside the fused silica substrate using a KOH solution (32 wt%) at 85 °C with ultrasound sonication (**Figure 7**).

5. Perform high-pressure testing

5.1. Saturate the microfluidic device with the resident fluid (e.g., DI water, surfactant solution, oil, etc. depending on the type of experiment) using a syringe pump.

5.2. Prepare foam-generating fluids and related instruments.

5.2.1. Prepare the brine solution (resident fluid) with the desired salinity and dissolve the surfactant (such as lauramidopropyl betaine and alpha-olefin-sulfonate) with the desired concentration (according to surfactant's critical micelle concentration) in the brine.

5.2.2. Fill the tanks of the CO_2 and water pumps with adequate amount of fluids per the experiment at room temperature.

5.2.3. Fill the brine accumulator and flow lines with the surfactant solution using a syringe. This work uses an accumulator with a capacity of 40 mL.

5.2.4. Rinse the brine line with the brine solution.

5.2.5. Rinse the line connecting the accumulator to the device and the outlet lines with the resident fluid (the brine solution in this case).

5.2.6. Place the saturated microfluidic device in a pressure-resistant holder and connect the inlet/outlet ports to the appropriate lines using 0.010" inner diameter tubing (**Figures 8**, **Supplementary File 1: Figure S5**).

5.2.7. Increase the temperature of the circulating bath, which controls the temperature of the brine and CO_2 lines, to the desired temperature (e.g., 40 °C here (**Figure 9**)).

5.2.8. Check all the lines to ensure the integrity of the setup prior to injection.

5.3. Generate the foam.

5.3.1. Begin injecting the brine at a rate of 0.5 mL/min and check the flow of surfactant solution into the device and the backpressure line.

5.3.2. Increase the backpressure and brine-pump pressure simultaneously in gradual steps (~ 0.006 MPa/s) while maintaining continuous flow from the outlet of the backpressure regulator (BPR). Increase the pressure up to ~7.38 MPa (minimum required $scCO_2$ pressure) and stop the pumps.

5.3.3. Increase the CO_2 line pressure up to a pressure above 7.38 MPa (minimum $scCO_2$ pressure).

5.3.4. Open the CO_2 valve and allow the $scCO_2$ mixed with the high-pressure surfactant solution to flow through an inline mixer to generate foam.

5.3.5. Wait until flow is fully developed inside the device and the channels are saturated. Monitor the outlet for the onset of foam generation.

NOTE: Auxiliary ports may be used to help pre-saturate the medium fully with the resident fluid (**Figure 1**). Inconsistencies in the rate of pressure build-up and sudden increases in BPR may lead to breakage (**Figure 10**). Fluid pressures and backpressure must be raised gradually to minimize the risk of damage to the device.

5.4. Perform real-time imaging and data analysis.

5.4.1. Turn on the camera to capture detailed images of flow inside the channels. This work uses a camera featuring a 60 megapixel, monochromatic, full-frame sensor.

5.4.2. Launch the dedicated shutter control software (**Table of Materials**). Select a shutter speed of 1/60, a focal ratio (f-number) of f/8.0, and select the appropriate lens.

5.4.3. Launch the dedicated camera software (**Table of Materials**). Select the camera, the desired format (e.g., IIQL) and an ISO setting of 200 in the pulldown menu under the "CAMERA" setting of the software.

5.4.4. Adjust the working distance of the camera to the medium as needed to focus on the medium. Capture images at prescribed time-intervals by pressing the **capture** button in the software.

5.5. Depressurize the system back to ambient conditions.

5.5.1. Stop injection (gas and liquid pumps), close the CO_2 and brine pump inlets, open the rest of the line valves and turn off the heaters.

5.5.2. Decrease the backpressure gradually (e.g., at a rate of 0.007 MPa/s) until the system reaches ambient pressure conditions. Decrease the brine and CO_2 pump pressures separately.

NOTE: Decreasing the $scCO_2$ pressure may result in inconsistent or turbulent BPR outflow, therefore the pressure drawdown must be executed with requisite care.

5.6. Clean the microfluidic device thoroughly after each experiment as needed by flowing the following sequence of solutions through the medium: isopropanol/ethanol/water (1:1:1), 2 M HCl solution, DI water, a basic solution (DI water/NH_4OH/H_2O_2 at 5:5:1) and DI water.

5.7. Post-process collected images.

5.7.1. Isolate the pore scape by excluding the background from the images.

5.7.2. Correct minor misalignments by performing perspective transformation and implementing a local thresholding strategy as needed to account for non-uniform illumination[28].

5.7.3. Calculate geometrical and statistical parameters relevant to the experiment such as average bubble size, bubble size distribution and bubble shape for each foam microstructural images in the channel.

REPRESENTATIVE RESULTS:

This section presents examples of physical observations from $scCO_2$ foam flow through a main fracture connected to array of micro-cracks. A glass microfluidic device made via photolithography or SLE is placed inside a holder and in the field of view of a camera featuring a 60 megapixel, monochromatic, full-frame sensor. **Figure 11** illustrates the process of fabrication microfluidic devices and their placement in the experimental setup. **Figure 12** is illustration of CO_2 foam transport and stability in the UV-lithography microfluidic device (4 MPa and 40 ˚C) during the first 20 min of generation/isolation. The multiphase moved across the fracture/microcracks and foam was generated through the microfractures. **Figure 13** shows $scCO_2$ foam generation in a SLE microfluidic device (7.72 MPa and 40 °C) starting from ambient condition with no flow to fully developed $scCO_2$ foam at high and low flow rates. **Figure 14** presents images of foam distribution and stability under reservoir conditions (7.72 MPa and 40 °C) during the first 20 min of generation/isolation. **Figure 15** shows the distribution of the bubble diameters and the raw and intermediate images as part of the quantification of the foam microstructure including, raw image, post-processed image with improved brightness, contrast and sharpness, and its binarized equivalent.

FIGURE LEGENDS:

Figure 1: Example photomask designs for fabrication of microfluidic devices (black and white colors are inverted for clarity). (**a**) Entire field of view for a connected fracture network containing a main fracture and micro cracks. (**b**) Zoomed-in view of the main feature comprising a connected fracture network containing a main fracture and micro-cracks. (**c**) A third port is added at the bottom. (**d**) Zoomed-in view of the main feature comprising a connected fracture network containing a main fracture and micro-cracks along with a distribution network connecting the network to the port at the bottom of the device.

Figure 2: 3D Microfludic design used in SLE fabrication and high-pressure foam flow through microchannels.

Figure 3: Examination of channel depth via confocal microscopy for substrate dipped in BD-etchant for 136 h (**no sonication in this case**)**.** (**a**) channel overview (**b**) channel depth measurement (~43 μm).

Figure 4: Examination of channel depth via confocal microscopy for a substrate with chrome layer removed after NMP rinsing. (**a**) Channel overview. (**b**) Channel depth measurement (~42.5 μm).

Figure 5: Schematic of thermal bonding process. (**a**) Placing two glass wafers between two smooth ceramic plates. (**b**) Placing the ceramic plates between two metallic plates and tightening the bolts. (**c**) Placing the metallic and ceramic holder containing the substrates inside a programmable furnace to achieve the desired temperatures for thermal bonding.

Figure 6: The completed UV-etched glass microfluidic device.

Figure 7: SLE design and fabrication process. (**a**) Schematic of SLE design and fabrication process (this figure has been reprinted with permission from Elsevier[27]), and (**b**) the resulting 3D printed microfluidic device. Design and fabrication steps include (**a.i**) designing the inner volume of channels, (**a.ii**) slicing the 3D model to create a z-stack of lines to define the laser path, (**a.iii**) laser irradiation on the polished fused silica substrate, (**a.iv**) preferential KOH etching of laser etched materials, and (**a.v**) the finished product.

Figure 8: Microfluidic device placed inside a holder and the imaging system comprising a high-resolution camera and an illumination system. (**a**) A photograph of laboratory setup, and (**b**) schematic of a lab-on-a-chip under observation via the high-resolution camera and illumination system.

Figure 9: High-pressure $scCO_2$ foam injection setup into a microfluidic device and a visualization system using a high-resolution camera and image processing unit; (**a**) photograph of laboratory setup, and (**b**) schematic of process flow diagram and the image processing unit.

Figure 10: De-bonded device at an injection port (right entrance) as a result of mishandling the pressure profile by BPR and water pump during injection.

Figure 11: Comparative fabrication methods of glass microfluidic device. (**a**) Fabrication process for fractured media microfluidic device using photo-lithography (**a.i**) design for a positive photoresist, (**a.ii**) printed photomask on a polyester-based transparency film, (**a.iii**) blank and photoresist/chrome coated glass substrates, (**a.iv**) transferring the pattern to the substrate via UV radiation, (**a.v**) etched substrate, (**a.vi**) etched substrate after chrome layer removal and the blank substrate prepared for thermal bonding, (**a.vii**) thermally bonded device, and (**a.viii**) $scCO_2$ injection. (**b**) Fabrication using the SLE technique: (**b.i**) design for SLE printing, (**b.ii**) laser

irradiation on the polished fused silica substrate, (**b.iii**) SLE printed glass microfluidic device, and (**b.iv**) $scCO_2$ injection.

Figure 12: CO_2 foam transport and stability in the UV-lithography microfluidic device (4 MPa and 40 ˚C) during the first 20 min of generation/isolation.

Figure 13: $scCO_2$ foam generation in the SLE microfluidic device (7.72 MPa and 40 °C). (**a**) Ambient condition with no flow through the micro channels. (**b**) Co-injection of CO_2 and aqueous phase (containing surfactant or nanoparticle) at supercritical condition. (**c**) Onset of $scCO_2$ foam generation 0.5 min after start of co-injection. (**d**) Fully developed $scCO_2$ foam at high flow rates (e) lowering the flow rates of co-injection to reveal the borders of multiphase. (**f**) Profoundly low flow rates reveal dispersed $scCO_2$ bubbles in the aqueous phase.

Figure 14: Visualization of foam stability under reservoir conditions (7.72 MPa and 40 ˚C) during the first 20 min of generation/isolation.

Figure 15: Analysis of foam microstructure. (**a**) Image of $scCO_2$ foam flow in the fracture network, (**b**) post-processed image with improved brightness, contrast and sharpness, (**c**) binarized image using ImageJ, and (**d**) bubble diameter distribution profile obtained from ImageJ, particle analysis mode.

Figure 16: Color-coded plot of UV intensity in a 10 x 10 cm^2 area of the stage where the substrate is placed for UV exposure. UV intensity values range from 4 to 5 mW/cm^2 as recorded using a UV meter.

Figure 17: Illustration of in-house collimated UV light source. (**a**) Photograph and (**b**) a schematic of laboratory UV light stand containing LED light sources and a stage.

DISCUSSION:

This work presents a protocol related to a fabrication platform to create robust, high-pressure glass microfluidic devices. The protocol presented in this work alleviates the need for a cleanroom by performing several of the final fabrication steps inside a glovebox. The use of a cleanroom, if available, is recommended to minimize the potential for contamination. Additionally, the choice of the etchant should be based on the desired surface roughness. The use of a mixture of HF and HCl as the etchant tends to reduce surface roughness[30]. This work is concerned with microfluidic platforms that enable direct, in situ visualization of transport of complex fluids in complex permeable media that faithfully represent the complex structures of subsurface media of interest. As such, this work uses a buffered etchant that enables the study of mass transfer and transport in surrogate media resembling geologic permeable media.

Design of patterns

The patterns are created using a computer aided design software (**Table of Materials**) and the features are intended to represent factures and microcracks to study transport and stability of foam (see **Figure 1**). These patterns may be printed on a high-contrast, polyester-based

transparent film, or a borofloat or quartz plate (photomask). The patterns used in photolithography comprise a main channel, 127 µm in width and 2.2 cm in length, that serves as the main fracture. This channel is connected to an array of micro-fractures with various dimensions, or a permeable medium consisting of an array of circular posts, with diameters of 300 µm, that are connected to the middle of the fracture path. Additional auxiliary ports may be included in the design to help with the initial saturation of the main features, e.g., fractures.

Photoresist

This work uses a positive photoresist. As a result, the areas in the design that correspond to features that are intended to be etched on the substrate are optically transparent and the other areas obstruct the transmission of light (collimated UV light). In the case of a negative photoresists, the situation would be the opposite: the areas in the design that correspond to the features that are intended to be etched on the substrate shall be optically nontransparent.

UV light source

The patterns are transferred to the photoresist by altering its solubility as a result of its exposure to UV light. A full-spectrum, mercury-vapor lamp may serve as the UV source. The use of a collimated, narrow-band UV source, however, improves the quality and precision of the fabrication significantly. This work uses a photoresist with peak sensitivity at 365 nm, a collimated UV source consisting of an array of light emitting diodes (LED), and an exposure time of approximately 150 s. This UV source is a developed in-house and offers a low maintenance, low-divergence, collimated UV light source for lithography. The UV source consists of a square array of nine high-power LEDs with a target peak emission wavelength of 365 nm at 25 °C (3.45 mm x 3.45 mm UV LED with Ceramic substrate—see **Table of Materials**). A light-collecting UV lens (LED 5 W UV Lens – see Table of Materials) is used on each LED to reduce the divergence from ~70° to ~12°. The divergence is further reduced (~5°) by using a 3 x 3 array of nine converging polyvinylchloride (PVC) Fresnel lenses. The setup produces collimated and uniform UV radiation over a 3.5-inch squared area. The details of the fabrication of this low-cost light source for UV lithography is adapted from the method presented by Erickstad and co-workers[25] with minor modifications[15,26]. **Figure 16** illustrates the LED UV light source mounted on the celling of UV stand alongside the stage at the bottom for substrate UV exposure (the procedure is performed in a darkroom). The UV stage is placed 82.55 cm from the nine Fresnel lenses that are mounted on a rack 13.46 cm below the rack that houses the LEDs. As seen in **Figure 16a**, there are four small fans (40 mm x 40 mm x 10 mm 12 V DC Cooling Fan—see **Table of Materials**) on the bottom of the plate that houses the LEDs and there is a larger fan (120 mm x 38 mm 24 V DC Cooling Fan—see **Table of Materials**) on the top. Three variable DC power supplies (**Table of Materials**) are used to power the LEDs. One power supply feeds the center LED at 0.15 A, 3.3 V; one power supply feeds the four corner LEDs at 0.6 A, 14.2 V; and one power supply feeds the remaining four LEDs at 0.3 A, 13.7 V. The stage, shown schematically in **Figure 16b**, is divided into 1 cm^2 sub-areas and the intensity of the UV light is measured in each using a UV power meter (**Table of Materials**) that is equipped with a 2 W 365 nm robe assembly. On average, the UV light has an average strength of 4.95 mW/cm^2 with a variability characterized by a standard deviation of 0.61 mW/cm^2. **Figure 17** presents a color-coded plot of UV intensity map for this UV light source. The intensity over the region of 10 cm × 10 cm is relatively uniform with values ranging from 4 to 5

613 mW/cm^2 in the center of the stage where the substrate is placed and exposed to the light. For
614 more information on the development of the in-house collimated UV-light source refer to ESI,
615 **Supplementary File 1: Figure S3, S4**. The use of the UV source may be coupled with UV blocking
616 shields/covers for its safe use. Additional safety measures may include the use of UV safety
617 goggles (Laser Eye Protection Safety Glasses for Red and UV Lasers – (190–400 nm)), face-shields
618 marked with the term Z87 that meets the ANSI standard (ANSI Z87.1-1989 UV certification) to
619 provide basic UV protection (**Table of Materials**) lab coats and gloves to minimize the exposure.
620
621 **Fabrication techniques**
622 This work also presents a step by step roadmap for high-pressure foam injection in fabricated
623 glass microfluidic devices using a high-resolution camera and an illumination source. Examples of
624 CO_2 and $scCO_2$ foam microstructure and transport in microfluidic devices are also presented with
625 relevance to fractured tight and ultra-tight formations. Direct observation of transport in these
626 subsurface media is a challenging task. As such, the devices described in this work provide an
627 enabling platform to study transport in permeable media under temperature and pressure
628 conditions that are relevant to subsurface applications such as fractured media, EOR processes
629 and aquifer remediation.
630
631 Devices used in this work are fabricated using two different techniques, namely
632 photolithography/wet-etching/thermal-bonding and SLE. The photolithography/wet-
633 etching/thermal-bonding technique comprises a relatively low-cost etching process using a low-
634 maintenance, collimated UV light-source. SLE is executed using a femto-second laser source
635 followed by removal of modified glass from the glass bulk via wet-etching. The main steps
636 involved in the photolithography/wet-etching/thermal-bonding technique include: (i) creation of
637 the map of the channel network, (ii) printing the design on polyester based transparency film or
638 a glass substrate, (iii) transferring the pattern on to a chrome/photoresist coated borosilicate
639 substrate, (iv) removal of exposed area by photo developer and chrome etchant solutions, (v)
640 etching the patterned area of the borosilicate substrate to the desired depth, (vi) preparing a
641 cover plate with entry holes positioned in appropriate locations, and (vii) thermal bonding of the
642 etched substrate and the cover plate. In contrast, SLE employs a two-step process: (i) selective
643 laser-induced printing in a transparent fused silica substrate, and (ii) selective removal of the
644 modified materials via wet chemical etching leading to the development of three-dimensional
645 features in the fused silica substrate. In the first step, laser radiation through the fused silica glass
646 internally modifies the glass bulk to increase the chemical/local etch-ability. The focused laser
647 scans inside the glass to modify a three-dimensional connected volume that is connected to one
648 of the surfaces of the substrate.
649
650 Both techniques result in devices that are chemically and physically resistant and tolerant of high
651 pressure and temperature conditions that correspond to subsurface systems of interest. Both
652 techniques provide pathways to create high-precision etched micro-channels and capable lab-
653 on-a-chip devices. The photolithography/wet-etching/thermal-bonding technique is robust in
654 terms of the geometry of the channels and may be used to etch complex channel networks,
655 whereas SLE is limited to relatively simple networks due to practical reasons. On the other hand,
656 devices made with photolithography/wet-etching/thermal-bonding may be more vulnerable to

breakage due to bonding imperfections, residual thermal stresses from fast heating/cooling rates during thermal bonding and structural flaws from the wet-etching process. In contrast to photolithography, SLE devices appear more resilient under high pressures (tested up to 9.65 MPa). Regardless of the fabrication technique, rapid pressure buildup rates may increase the chance of mechanical failures in microfluidic devices.

ACKNOWLEDGMENTS:

The authors from the University of Wyoming gratefully acknowledge support as part of the Center for Mechanistic Control of Water-Hydrocarbon-Rock Interactions in Unconventional and Tight Oil Formations (CMC-UF), an Energy Frontier Research Center funded by the U.S. Department of Energy, Office of Science under DOE (BES) Award DE-SC0019165. The authors from the University of Kansas would like to acknowledge the National Science Foundation EPSCoR Research Infrastructure Improvement Program: Track -2 Focused EPSCoR Collaboration award (OIA- 1632892) for funding of this project. Authors also extend their appreciation to Jindi Sun from the Chemical Engineering Department, University of Wyoming for her generous help in instrument training. SAA thanks Kyle Winkelman from the University of Wyoming for his help with constructing the imaging and UV stands. Last but not the least, the authors gratefully acknowledge John Wasserbauer from microGlass, LLC for useful discussions regarding the SLE technique.

DISCLOSURES:

The authors declare no conflicts of interest and disclosure.

REFERENCES:

1 Hyman, J.D. et al. Understanding hydraulic fracturing: a multi-scale problem. *Philosophical Transactions of the Royal Society A: Mathematical, Physical and Engineering Sciences A*. **13**(374), 1-15 (2016).

2 Middleton R.S. et al. Shale gas and non-aqueous fracturing fluids: Opportunities and challenges for supercritical CO_2. *Applied Energy*. **147** (1), 500-509 (2015).

3 Hosseini, H, Tsau, J., Peltier, E., Barati, R. Lowering Fresh Water Usage in Hydraulic Fracturing by Stabilizing $scCO_2$ Foam with Polyelectrolyte Complex Nanoparticles Prepared in High Salinity Produced Water. *SPE-189555-MS.* (2018).

4 Gregory, K.B., Vidic, R.D., Dzombak, D.A. Water management challenges associated with the production of shale gas by hydraulic fracturing. *Elements*. **7**,181–186.(2017).

5 Ellsworth W.L. Injection-Induced Earthquakes **341**, 1–8 (2013).

6 Hosseini, H. et al. Experimental and Mechanistic Study of Stabilized Dry CO_2 Foam Using Polyelectrolyte Complex Nanoparticles Compatible with Produced Water To Improve Hydraulic Fracturing Performance. *Journal of Industrial and Engineering Chemistry Research*. **58**, 9431−9449 (2019).

7 Hosseini, H., Tsau, J.S., Peltier, E., Ghahfarokhi, R.B. Highly stable $scCO_2$-high salinity brine interface for waterless fracturing using polyelectrolyte complex nanoparticles. *Abstract Paper of American Chemical Society*. **256**, Boston, MA, ACS (2018).

8 Al-Muntasheri, G.A. Critical Review of Hydraulic-Fracturing Fluids for Moderate- to Ultralow- Permeability Formations Over the Last Decade. *SPE Production & Operations*, *SPE-169552-PA*. **29**, (04), 243-260 (2014).
9 Tong, S., Singh, R., Mohanty, K.K. Proppant Transport in Fractures with Foam-Based Fracturing Fluids. *SPE-187376-MS.* (2017).
10 Fernø, M.A., Eide, Ø., Steinsbø, M., Langlo, S.A.W, Christophersen, A., Skibenes, A., et al. Mobility control during CO_2 EOR in fractured carbonates using foam: Laboratory evaluation and numerical simulations. *Journal of Petroleum Science and Engineering.* **135**, 442–51 (2015).
11 Middleton R., Viswanathan H., Currier, R., Gupta, R. CO_2 as a fracturing fluid: Potential for commercial-scale shale gas production and CO_2 sequestration. *Energy Procedia.* **63**, 7780–7784 (2014).
12 Guo, F., Aryana, S.A. Improved sweep efficiency due to foam flooding in a heterogeneous microfluidic device. *Journal of Petroleum Science and Engineering*. **164**, 155–163 (2018).
13 Nazari, N., Hosseini, H., Jyun-Syung, T., Shafer-Peltier, K., Marshall, C., Ye, Q., Ghahfarokhi, R.B. Development of Highly Stable Lamella Using Polyelectrolyte Complex Nanoparticles: An Environmentally Friendly scCO_2 Foam Injection Method for CO_2 Utilization Using EOR. *Fuel.* **261,** 11636 (2020).
14 Nguyen, V.H., Kang, C., Roh, C., Shim, J.J. Supercritical CO_2 -Mediated Synthesis of CNT@Co_3O_4 Nanocomposite and Its Application for Energy Storage. *Industrial and Engineering Chemistry Research.* **55**, 7338−7343 (2016).
15 Guo, F., Aryana, S.A., Wang, Y., Mclaughlin, J.F., Coddington, K. Enhancement of storage capacity of CO_2 in megaporous saline aquifers using nanoparticle-stabilized CO_2 foam. *International Journal of Greenhouse Gas Control*. **87**, 134–141 (2019).
16 Guo, F., Aryana, S. An experimental investigation of nanoparticle-stabilized CO_2 foam used in enhanced oil recovery. *Fuel.* **186**, 430–42 (2016).
17 Guo, F., He, J., Johnson, A., Aryana, S.A. Stabilization of CO_2 foam using by-product fly ash and recyclable iron oxide nanoparticles to improve carbon utilization in EOR processes. *Sustainable Energy and Fuels*. **1**, 814–22 (2017).
18 Wang, Y., Shahvali, M. Discrete fracture modeling using Centroidal Voronoi grid for simulation of shale gas plays with coupled nonlinear physics. *Fuel*. **163**, 65–73 (2016).
19 Tiggelaar, R. M., Benito-Lopez, F., Hermes, D.C., Rathgen, H., Egberink, R.J.M., Mugele, F.G., Reinhoudt, N.D., van den Berg, A., Verboom, W., Gardeniers, H.J.G.E. Fabrication, mechanical testing and application of high-pressure glass microreactor chips. *Chemical Engineering Journal*. **131**, 163–170 (2007).
20 Marre, S., Adamo, A., Basak, S., Aymonier, C. Jensen, K. F. Design and Packaging of Microreactors for High Pressure and High Temperature Applications. *Industrial and Engineering Chemistry Research.* **49**, 11310–11320 (2010).
21 Paydar, O. H., Paredes, C. N., Hwang, Y., Paz, J., Shah, N.B., Candler, R.N. Characterization of 3D-printed microfluidic chip interconnects with integrated O-rings. *Sensors Actuators A: Physical.* **205,** 199–203 (2014).
22 Jiménez-Martínez, J. et al. Pore-scale mechanisms for the enhancement of mixing in unsaturated porous media and implications for chemical reactions. *Geophysical Research Letters.* **42**, 5316–5324 (2015).

23 Jiménez-martínez, J., Porter, M.L., Hyman, J.D., Carey, J.W., Viswanathan, H.S. Mixing in a three-phase system: Enhanced production of oil-wet reservoirs by CO_2 injection. *Geophysical Research Letters.* **43**, 196–205 (2016).
24 Rognmo, A. U., Fredriksen, S. B., Alcorn, Z. P. Pore-to-Core EOR Upscaling for CO_2 Foam for CCUS. *SPE Journal*. **24**, 1-11 (2019).
25 Erickstad, M., Gutierrez, E., Groisman, A low-cost low-maintenance ultraviolet lithography light source based on light-emitting diodes. *Lab on a Chip.* **15**, 57–61 (2015).
26 Guo, F., Aryana, S.A. An Experimental Investigation of Flow Regimes in Imbibition and Drainage Using a Microfluidic Platform. *Energies*. **12**(7), 1390, 1–13 (2019).
27 Burshtein, N., Chan, S.T., Toda-peters, K., Shen, A.Q., Haward S.J. 3D-printed glass microfluidics for fluid dynamics and rheology. *Current Opinion in Colloid & Interface Science*. **43**, 1–14 (2019).
28 Wang, Y., Aryana, S.A. Creation of Saturation Maps from Two-Phase Flow Experiments in Microfluidic Devices. In *Advances in Petroleum Engineering and Petroleum Geochemistry. Advances in Science, Technology & Innovation.* Edited by Banerjee, S., Barati, R., Patil, S. 77–80, Springer (2019).
29 Hermans, M., Gottmann, J., Riedel, F. Selective, Laser-Induced Etching of Fused Silica at High Scan-Speeds Using KOH. *Journal of Laser Micro/Nanoengineering*, 9, 126–131 (2014).
30 Iliescu, C., Jing, J., Tay, F.E.H., Miao, J., Sun, T. Characterization of masking layers for deep wet etching of glass in an improved HF/HCl solution. *Surface & Coatings Technology*. **198**, 314–318 (2005).

Figure 1

Click here to access/download;Figure;Figure 1.tif

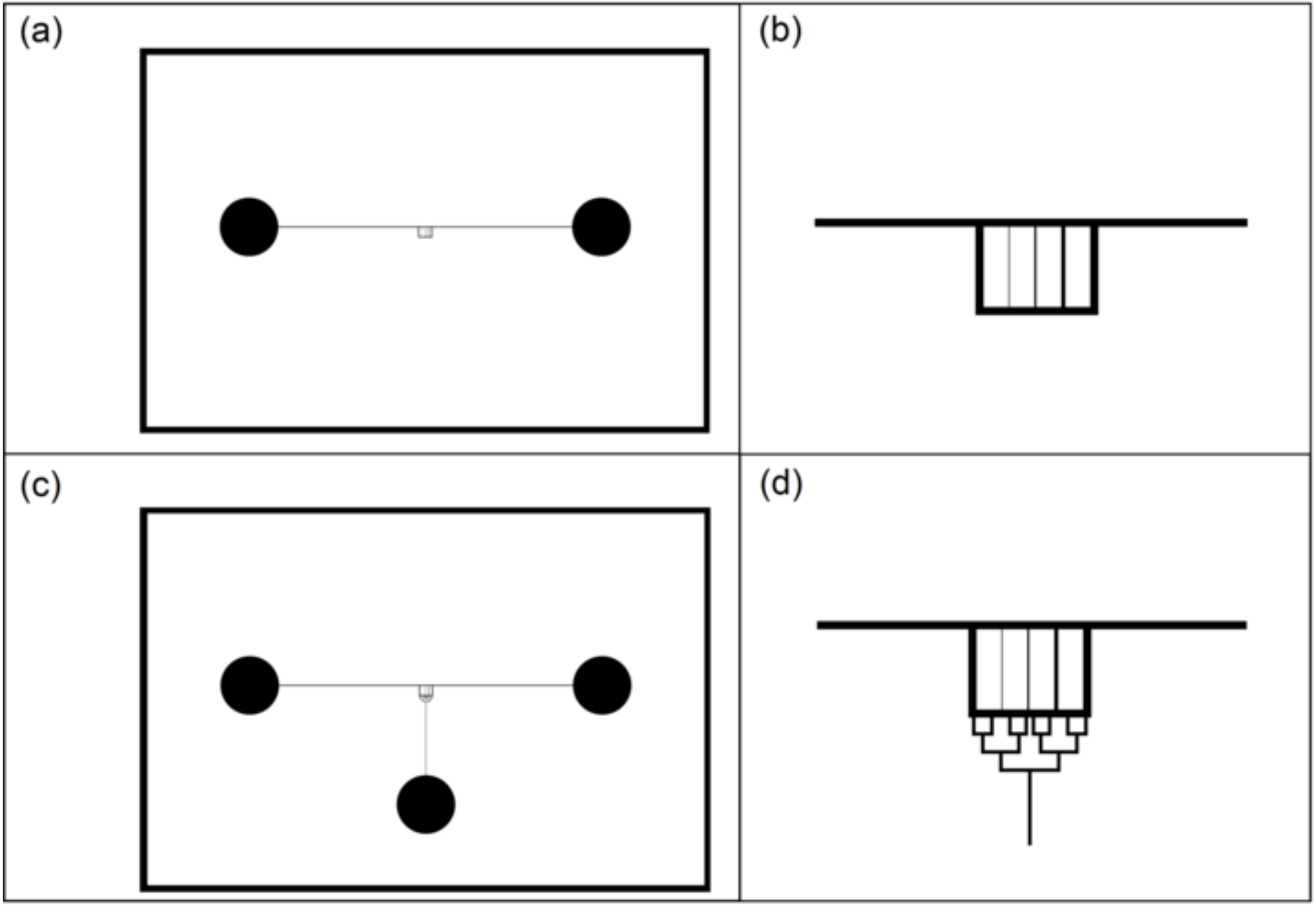

Figure 2

Click here to access/download;Figure;Figure 2.tif

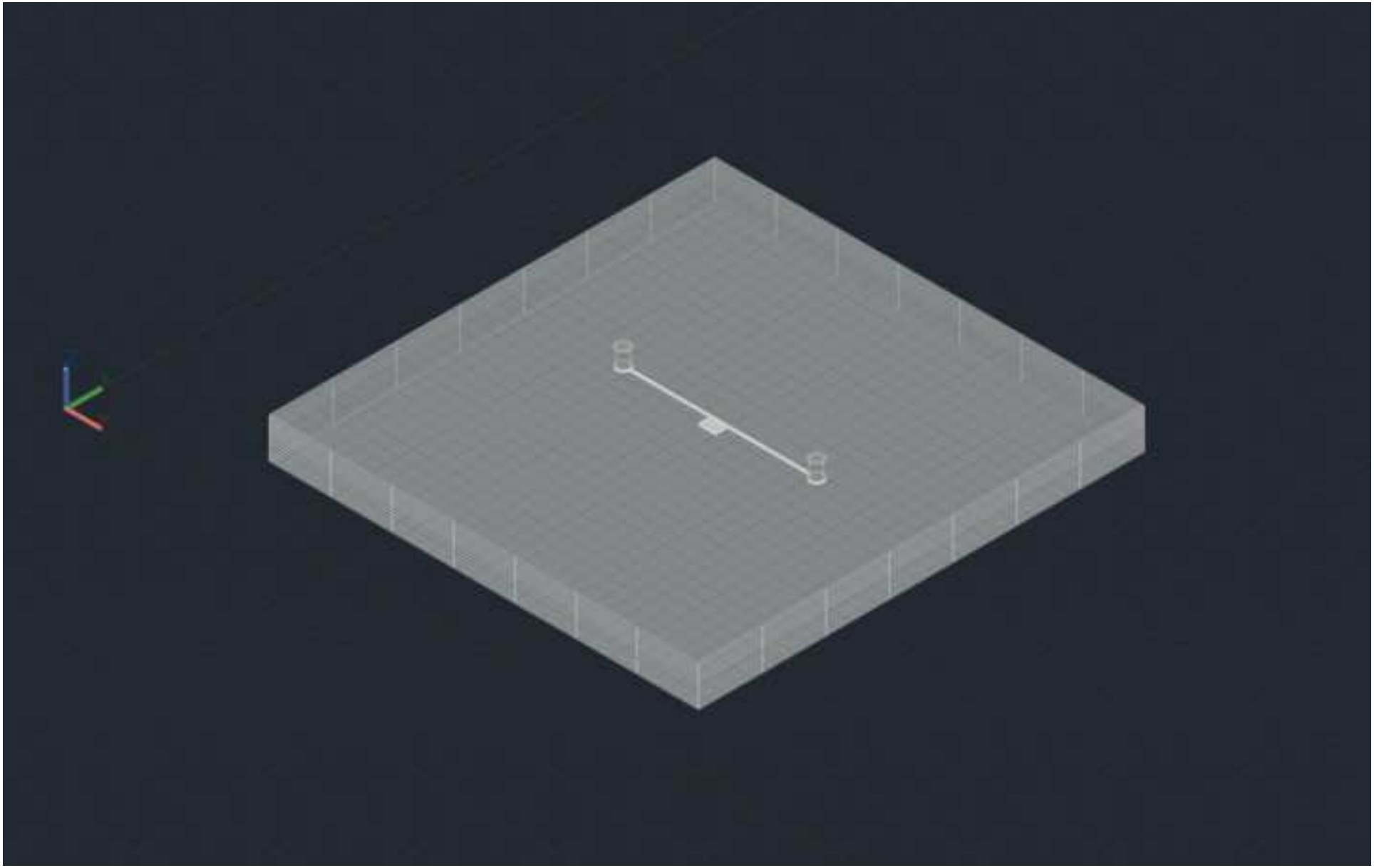

Figure 3

Click here to access/download;Figure;Figure 3.tif

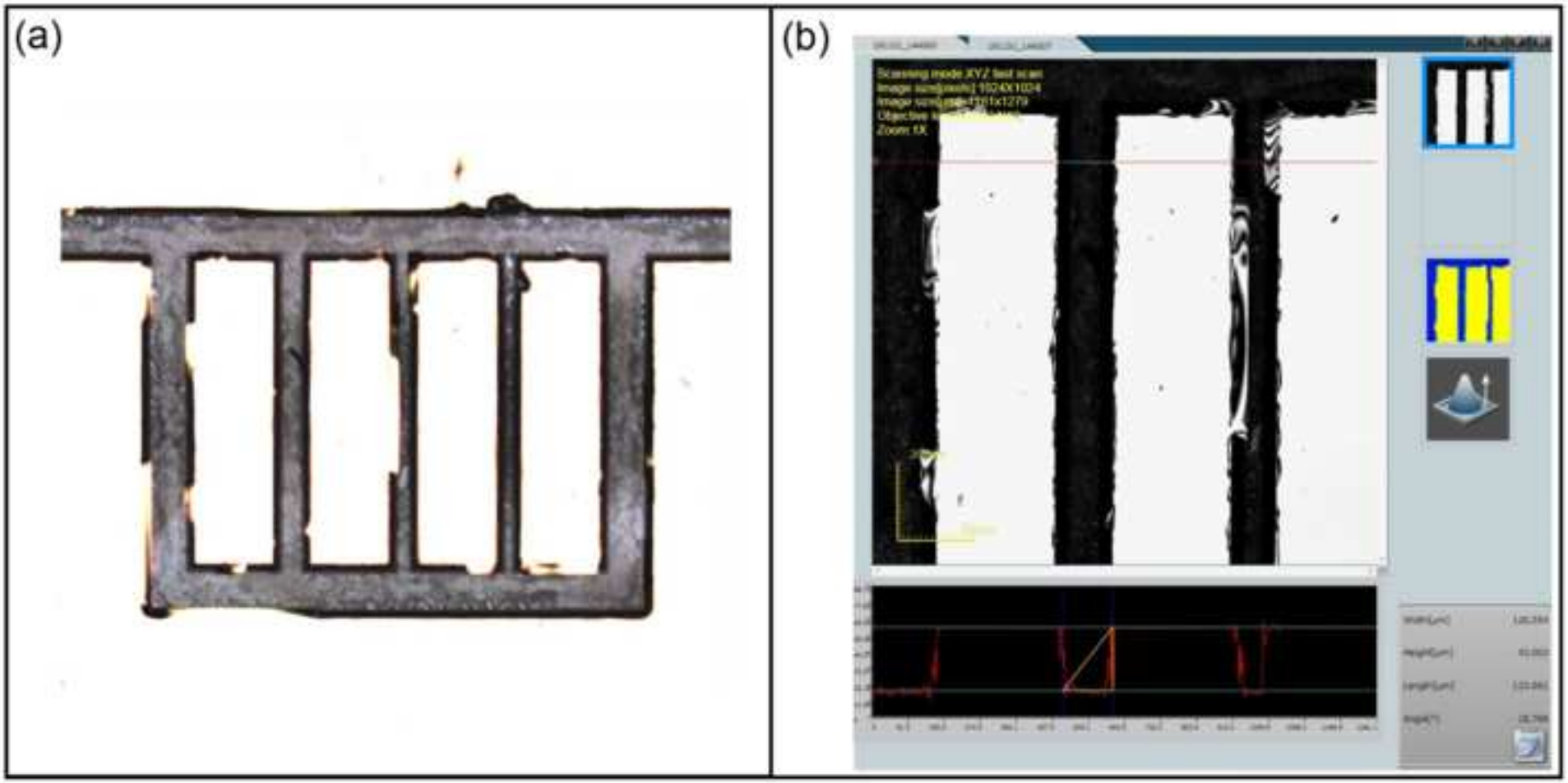

Figure 4

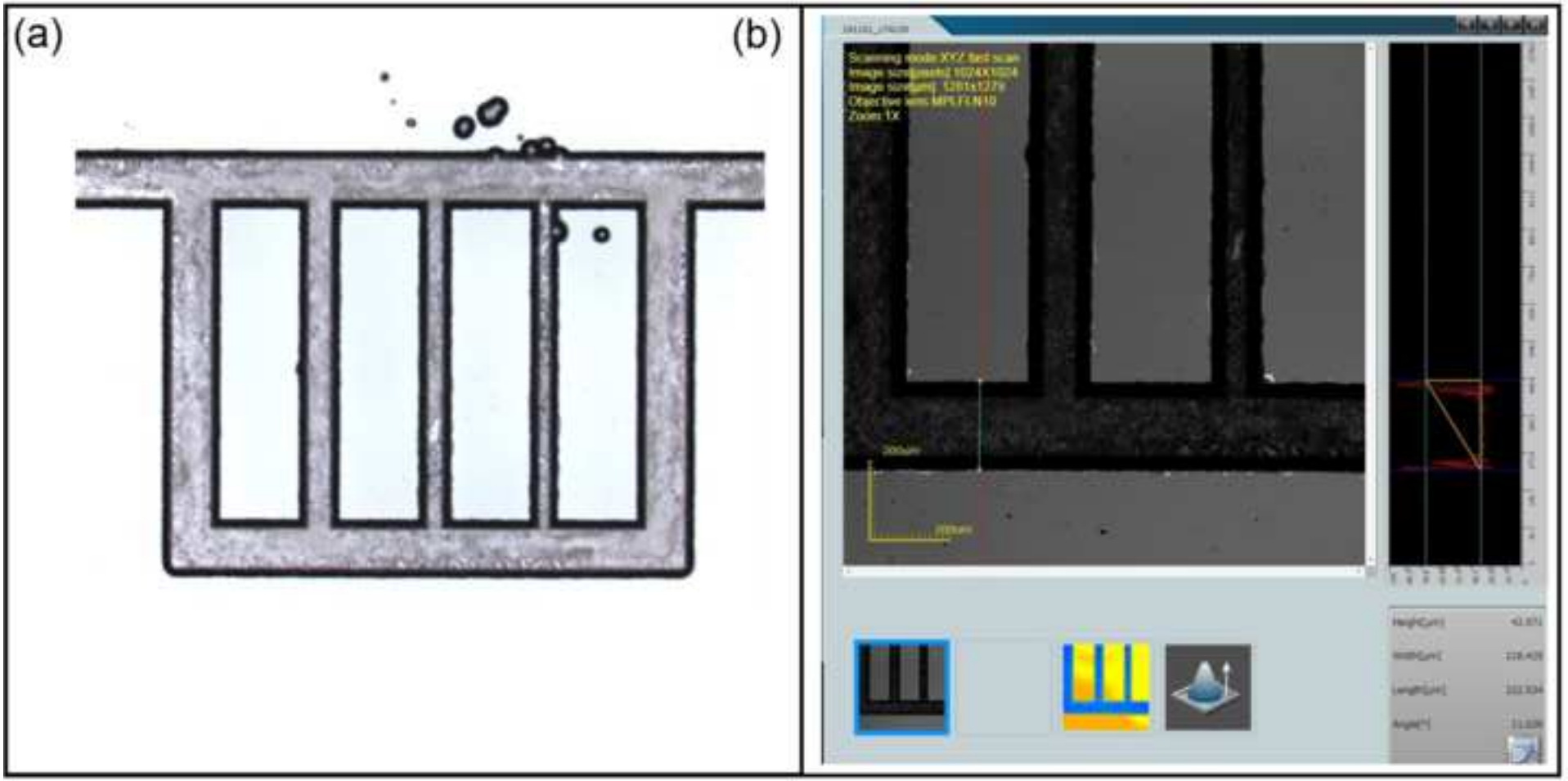

Figure 5

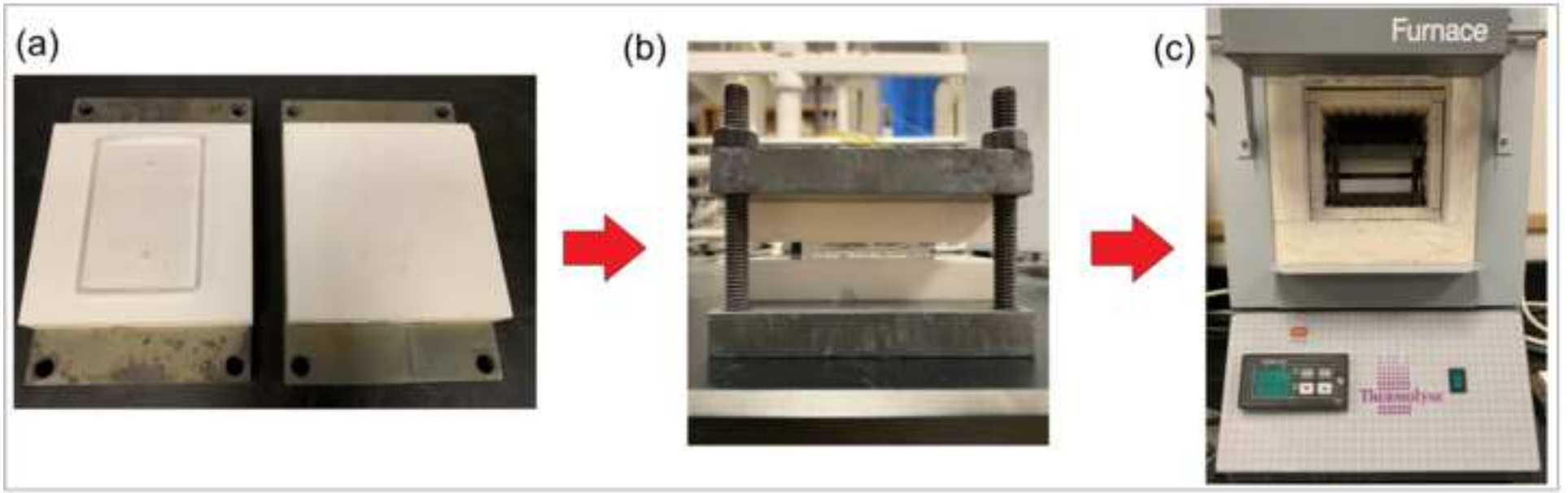

Figure 6

Click here to access/download;Figure;Figure 6.tif

Figure 7

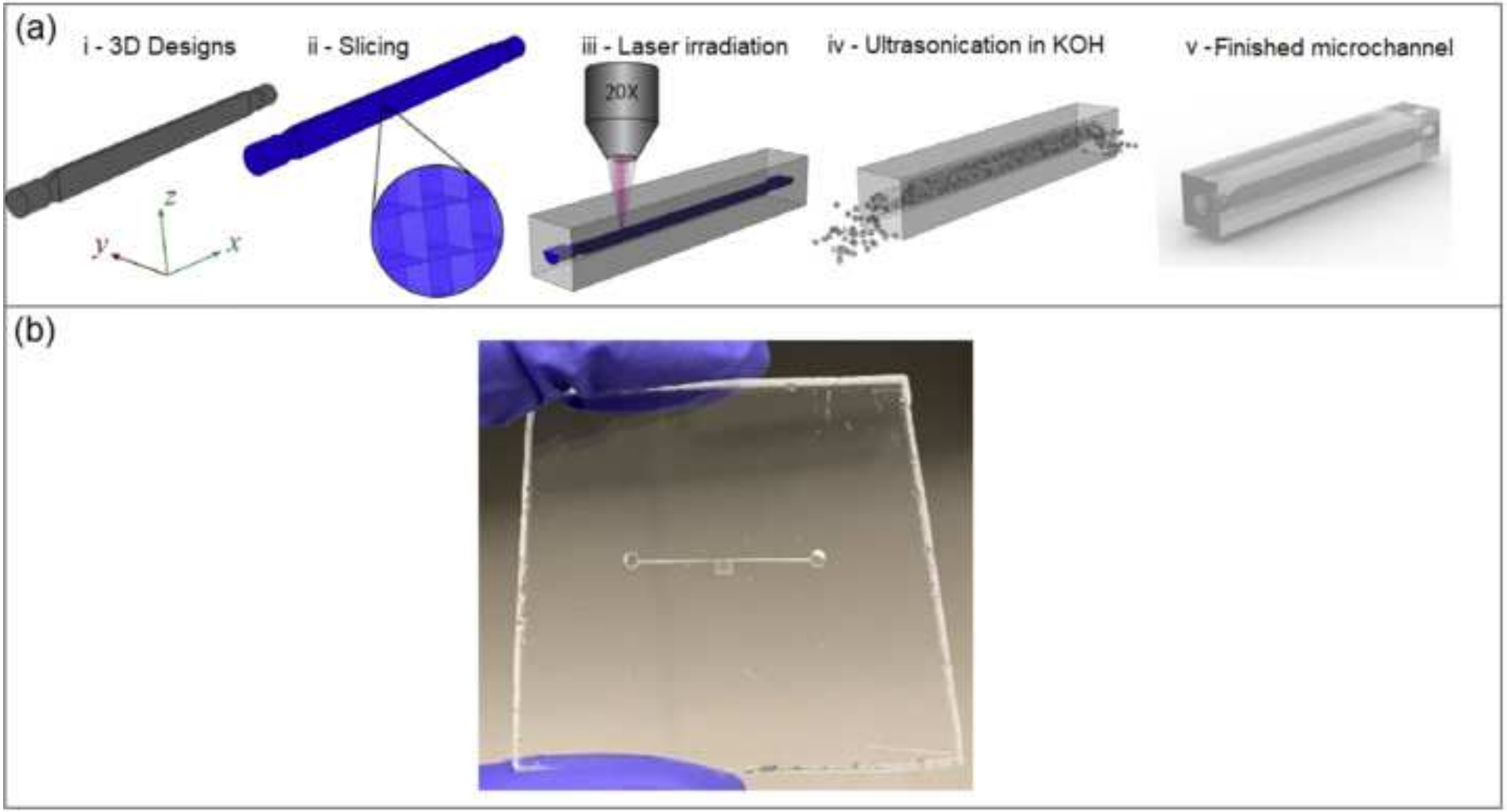

Figure 8

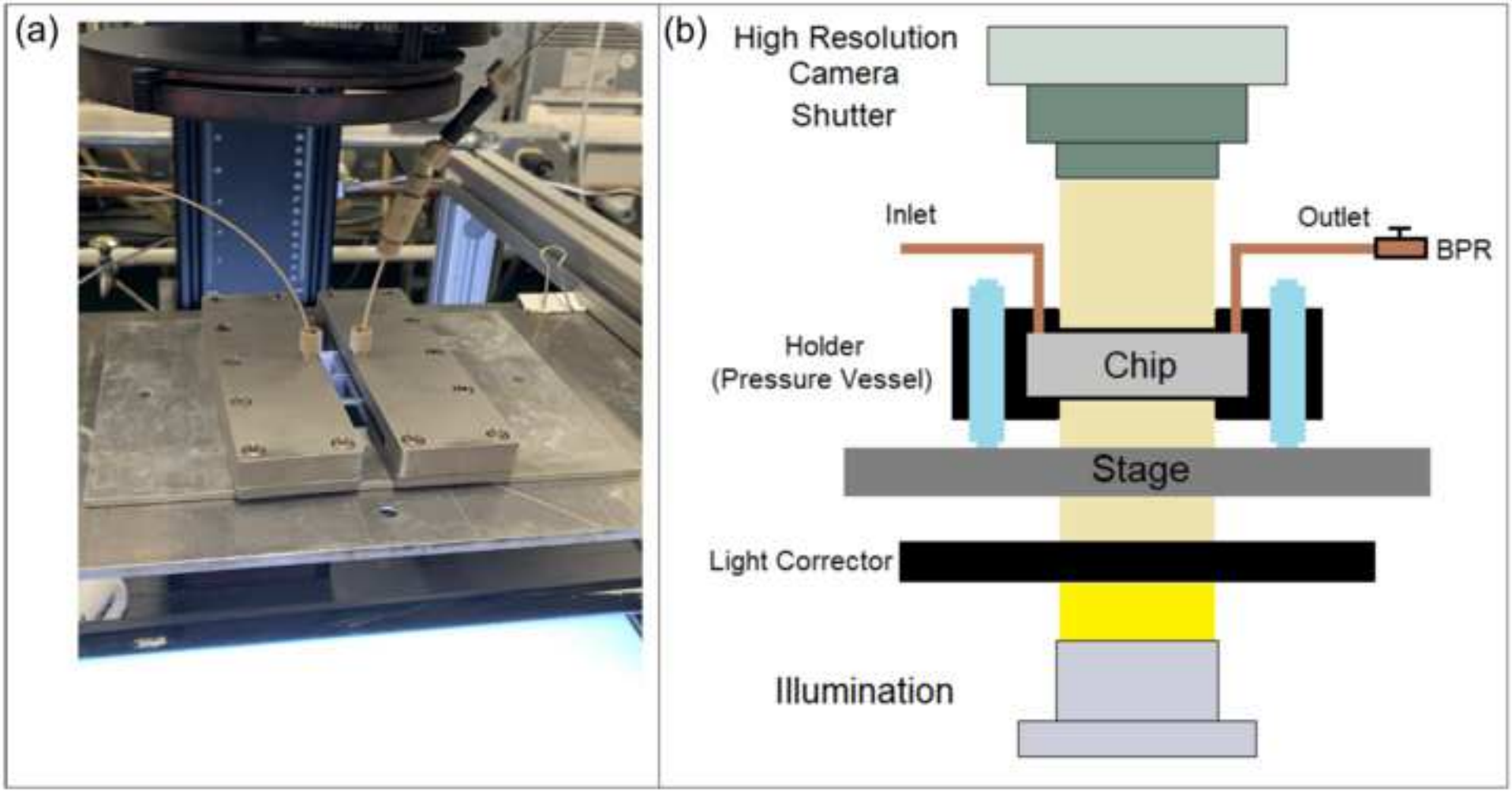

Figure 9

Click here to access/download;Figure;Figure 9.tif

Figure 10

Click here to access/download;Figure;Figure 10.tif

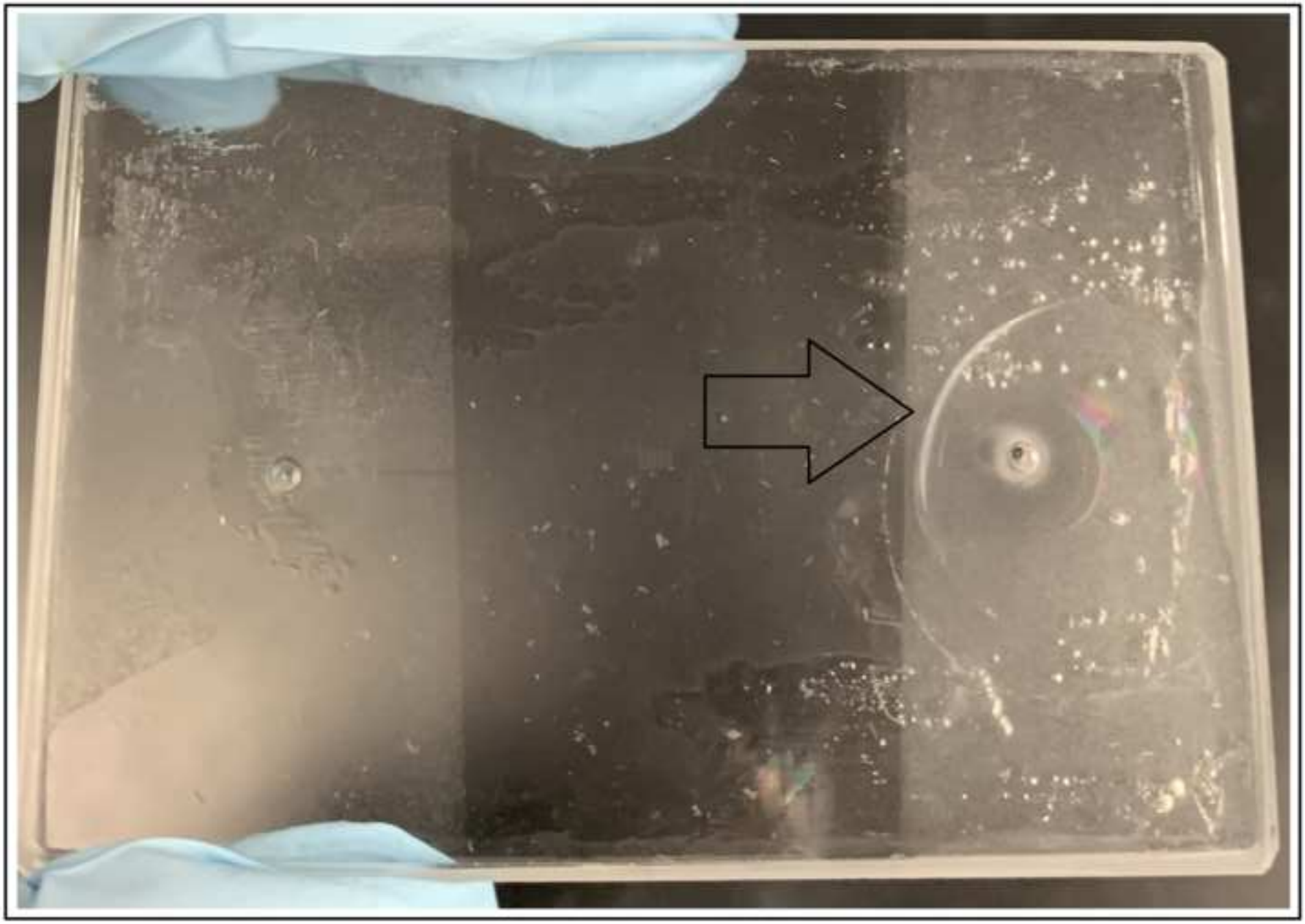

Figure 11

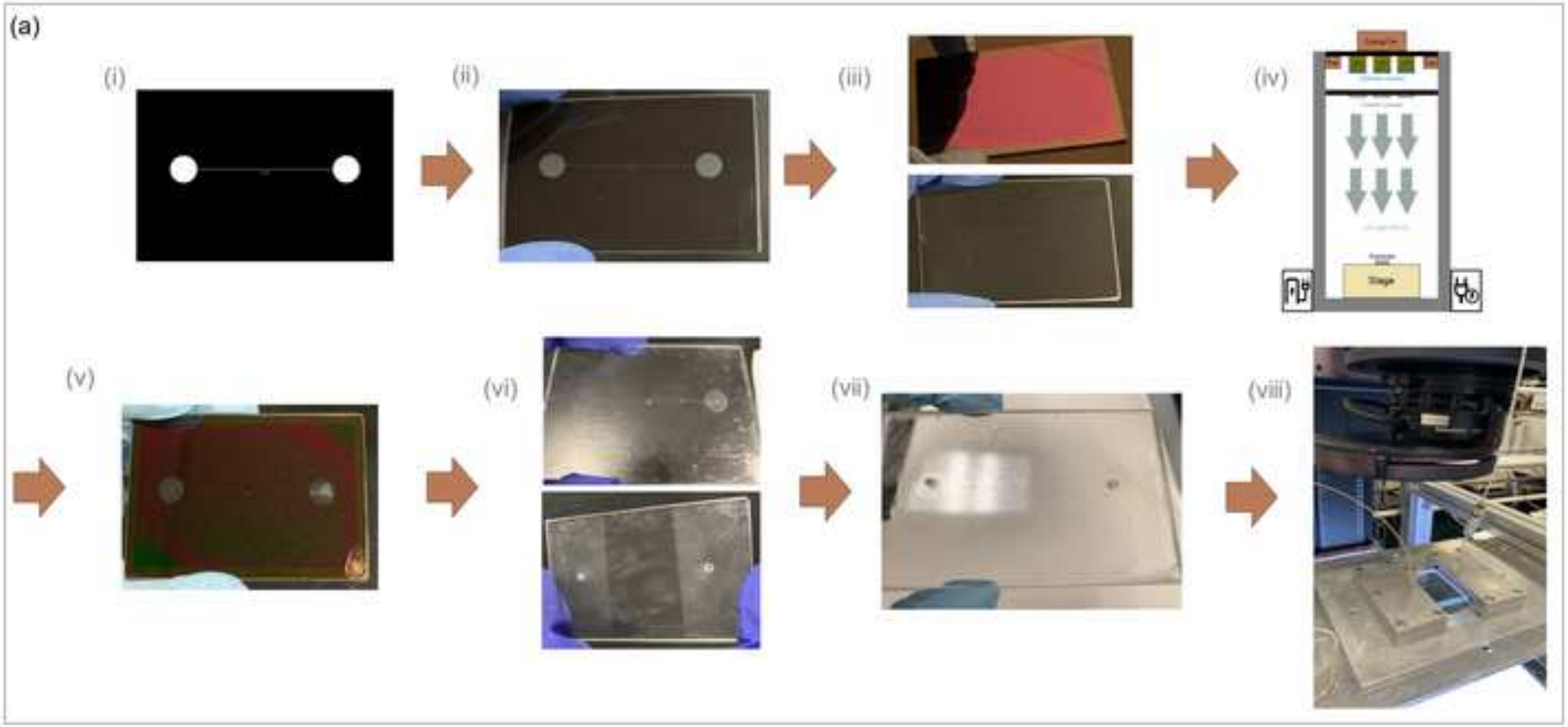

Figure 12

Click here to access/download;Figure;Figure 12.tif

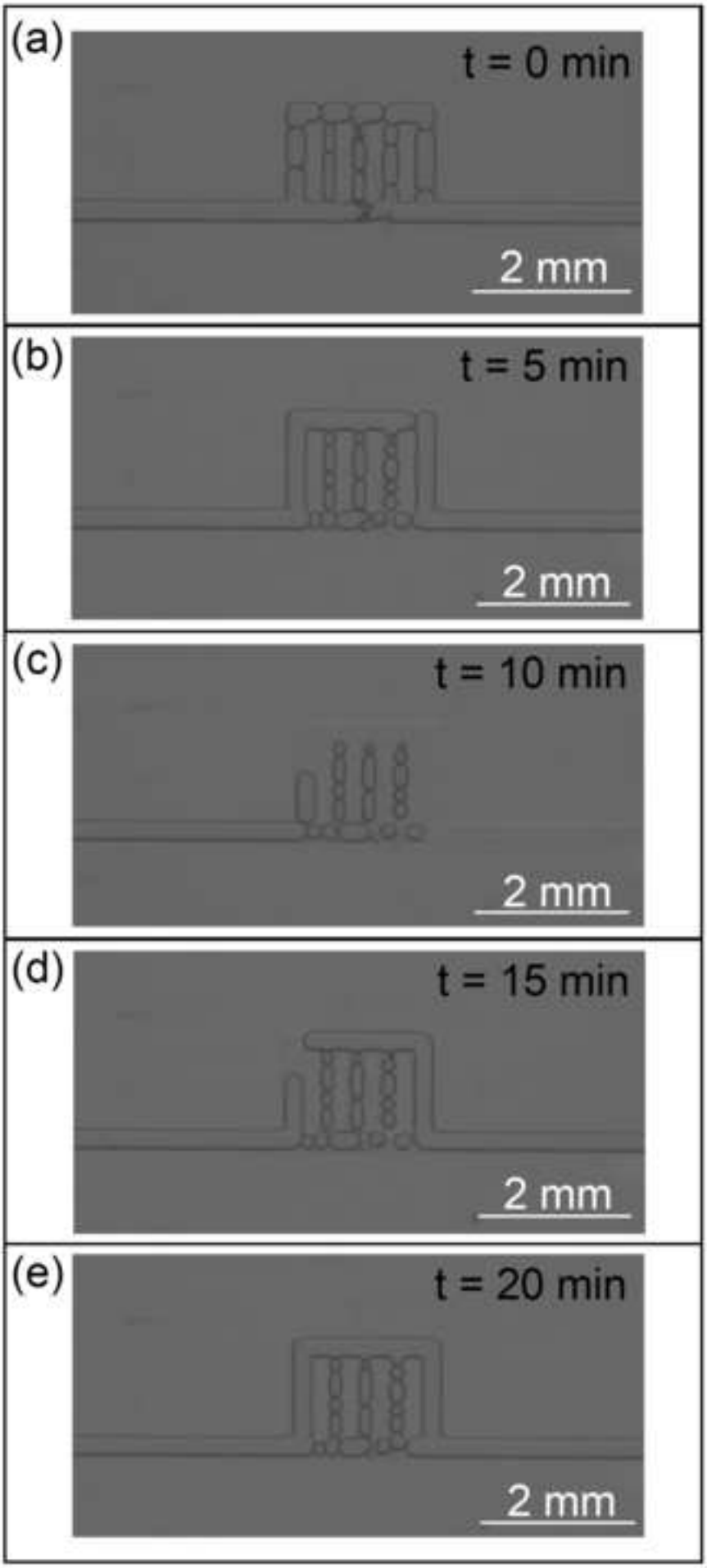

Figure 13

Click here to access/download;Figure;Figure 13.tif

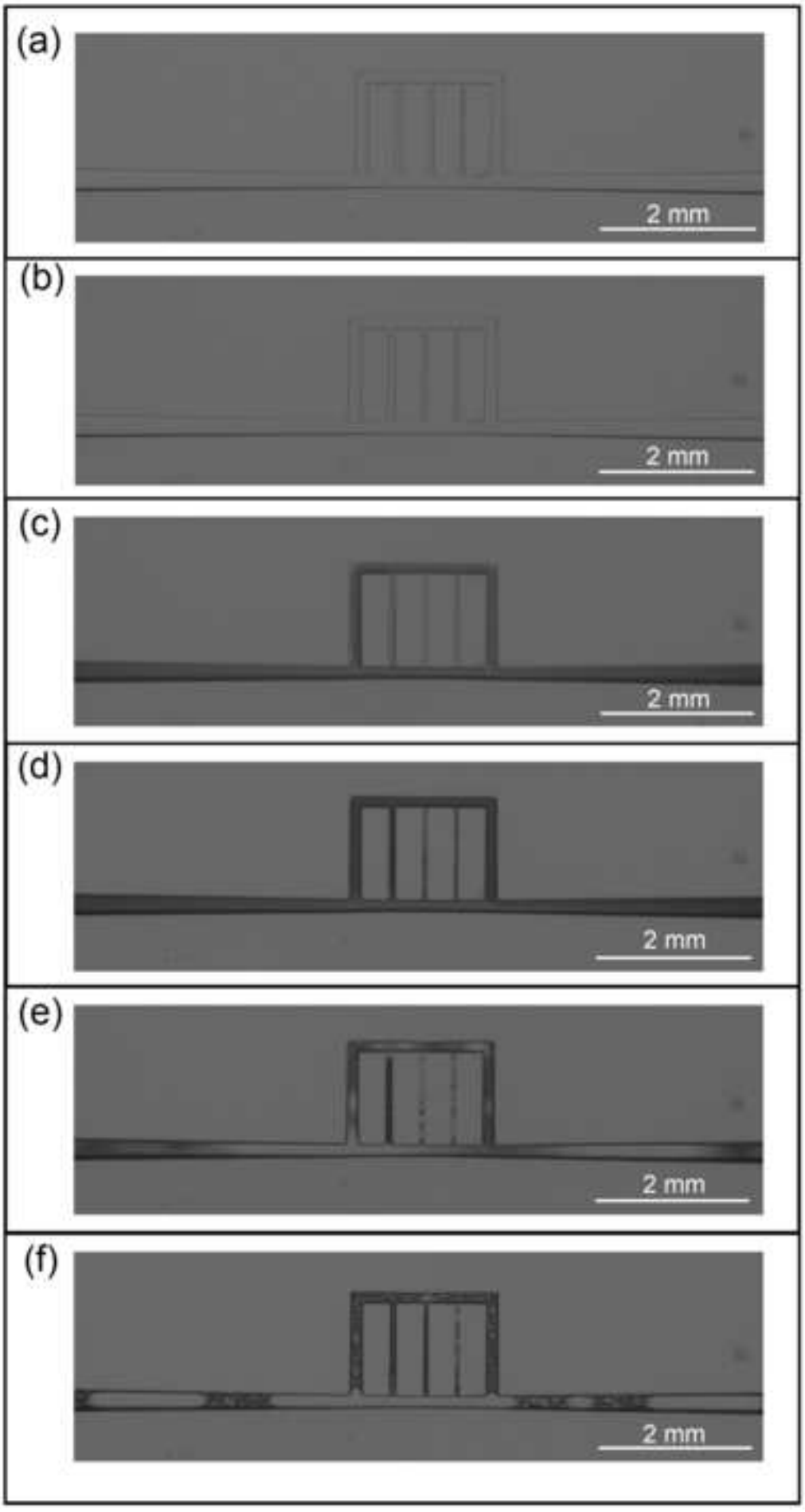

Figure 14

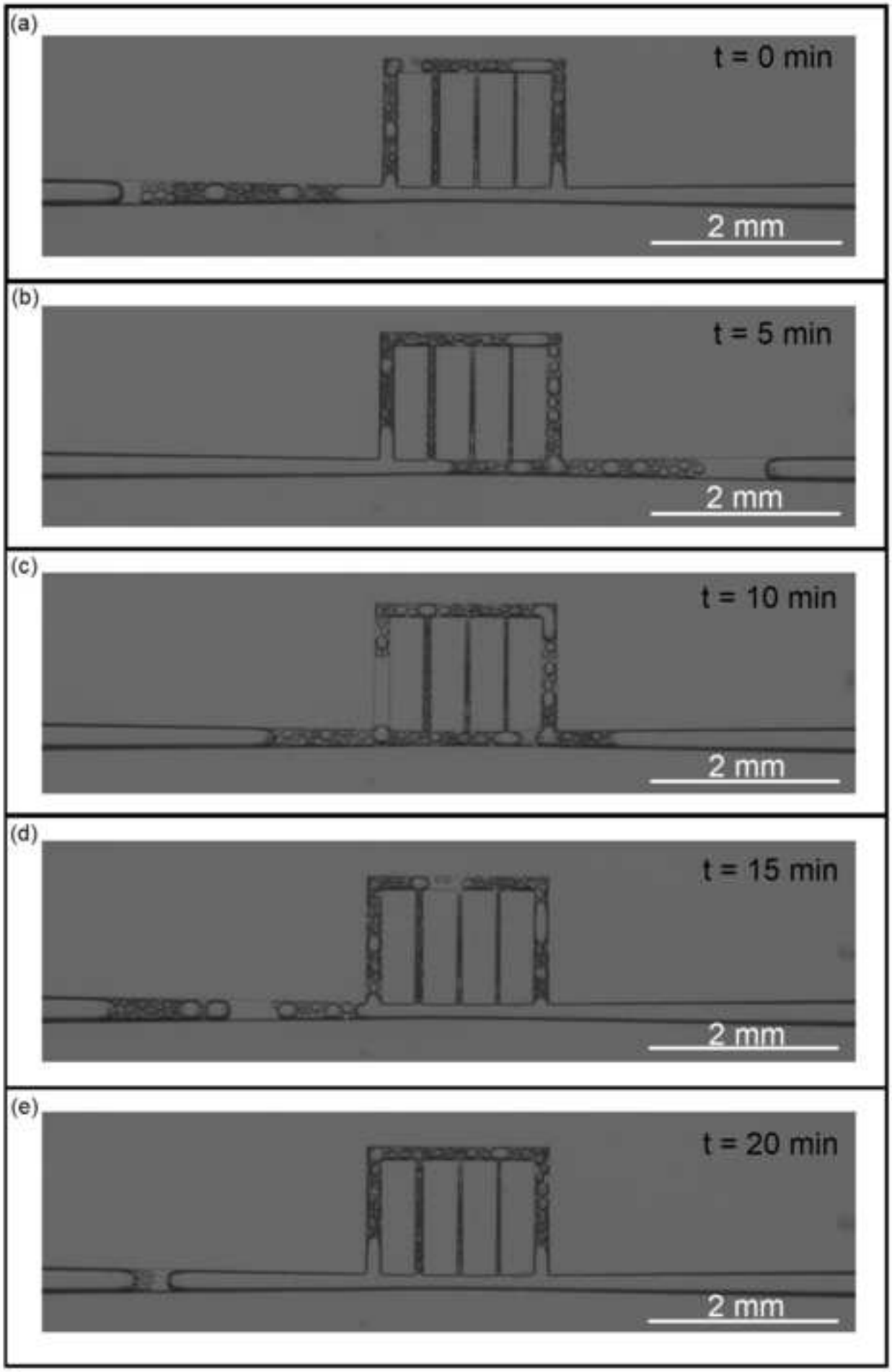

Figure 15

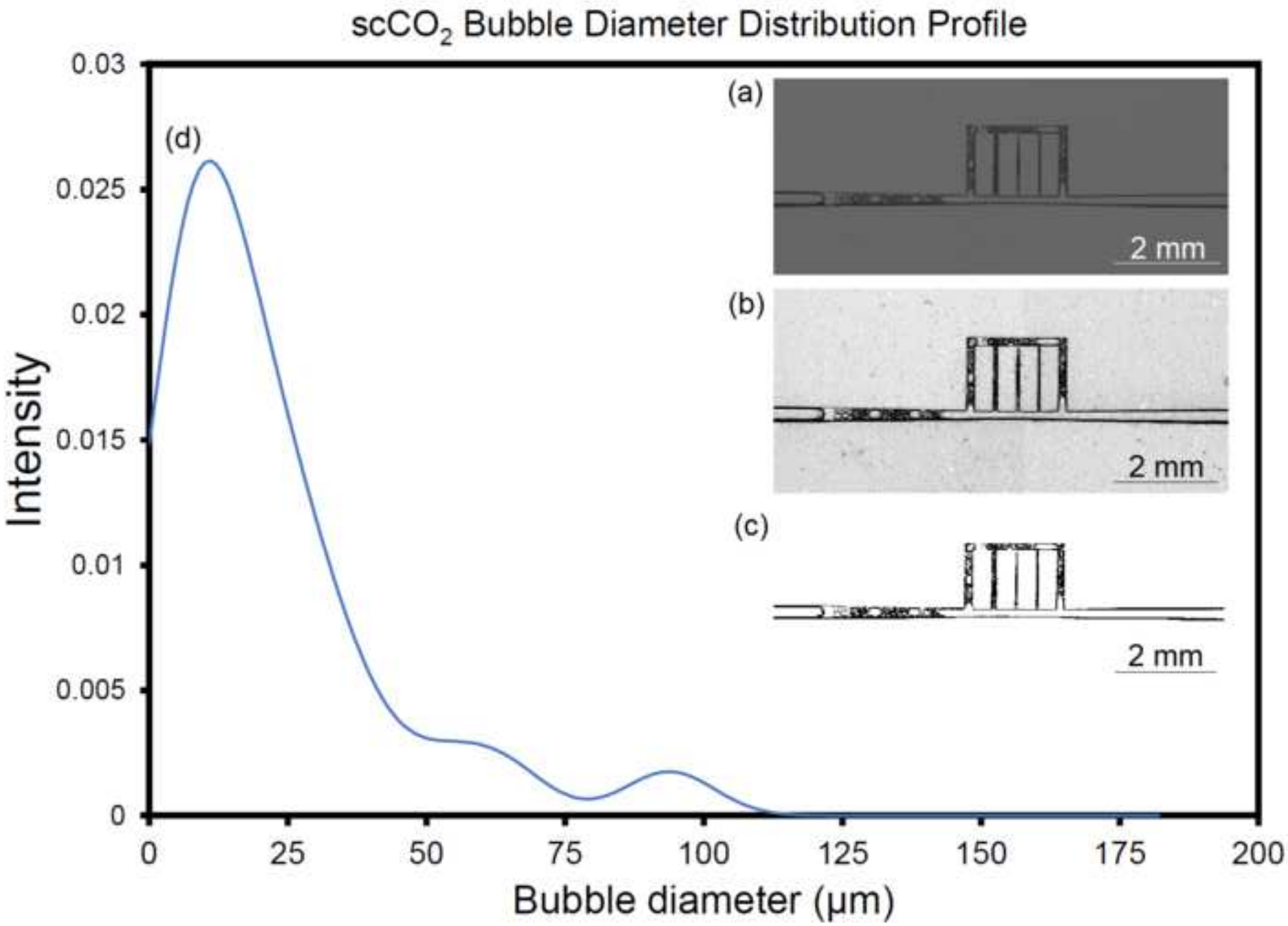

Figure 16

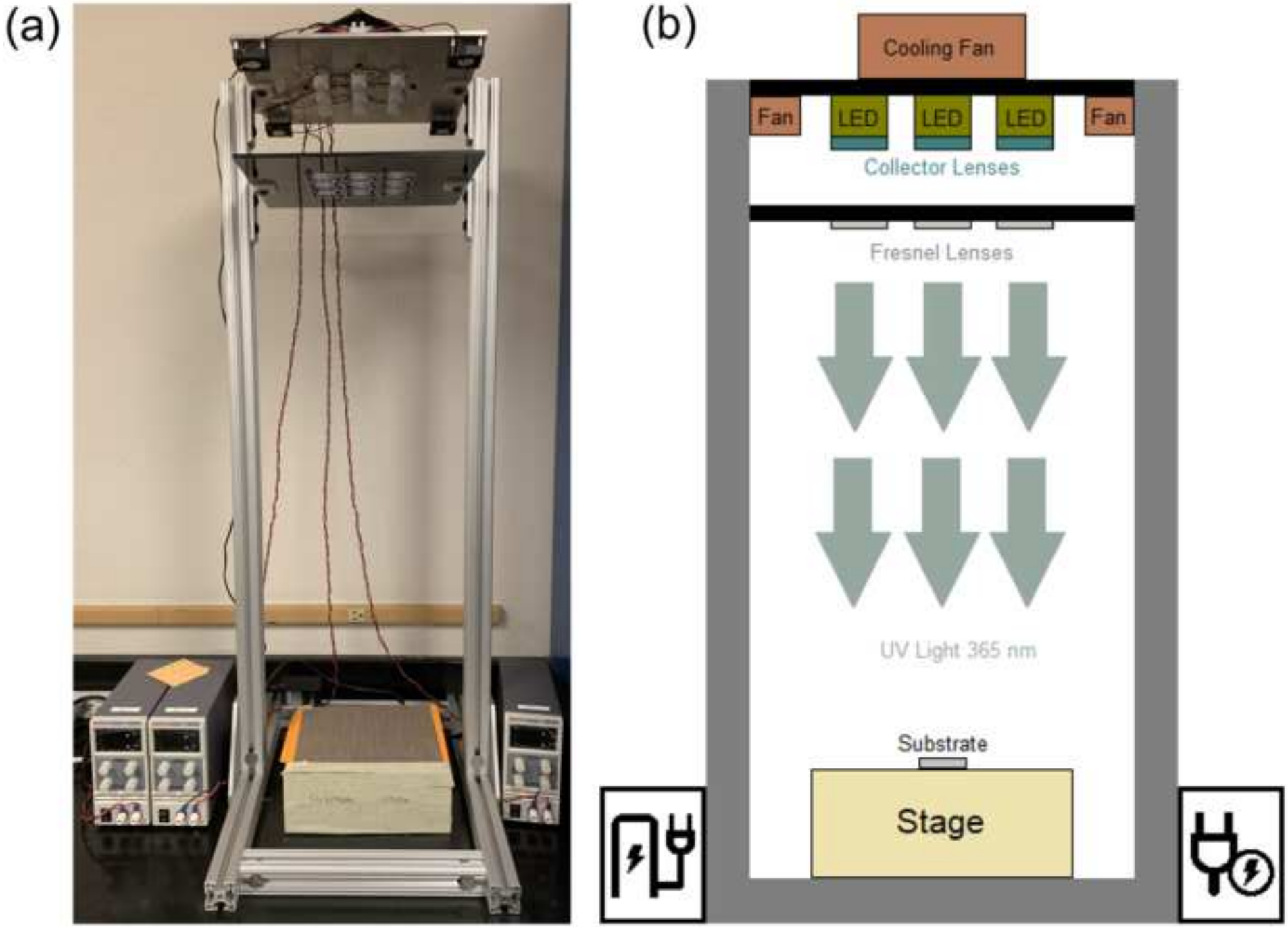

Figure 17

Click here to access/download;Figure;Figure 17.tif

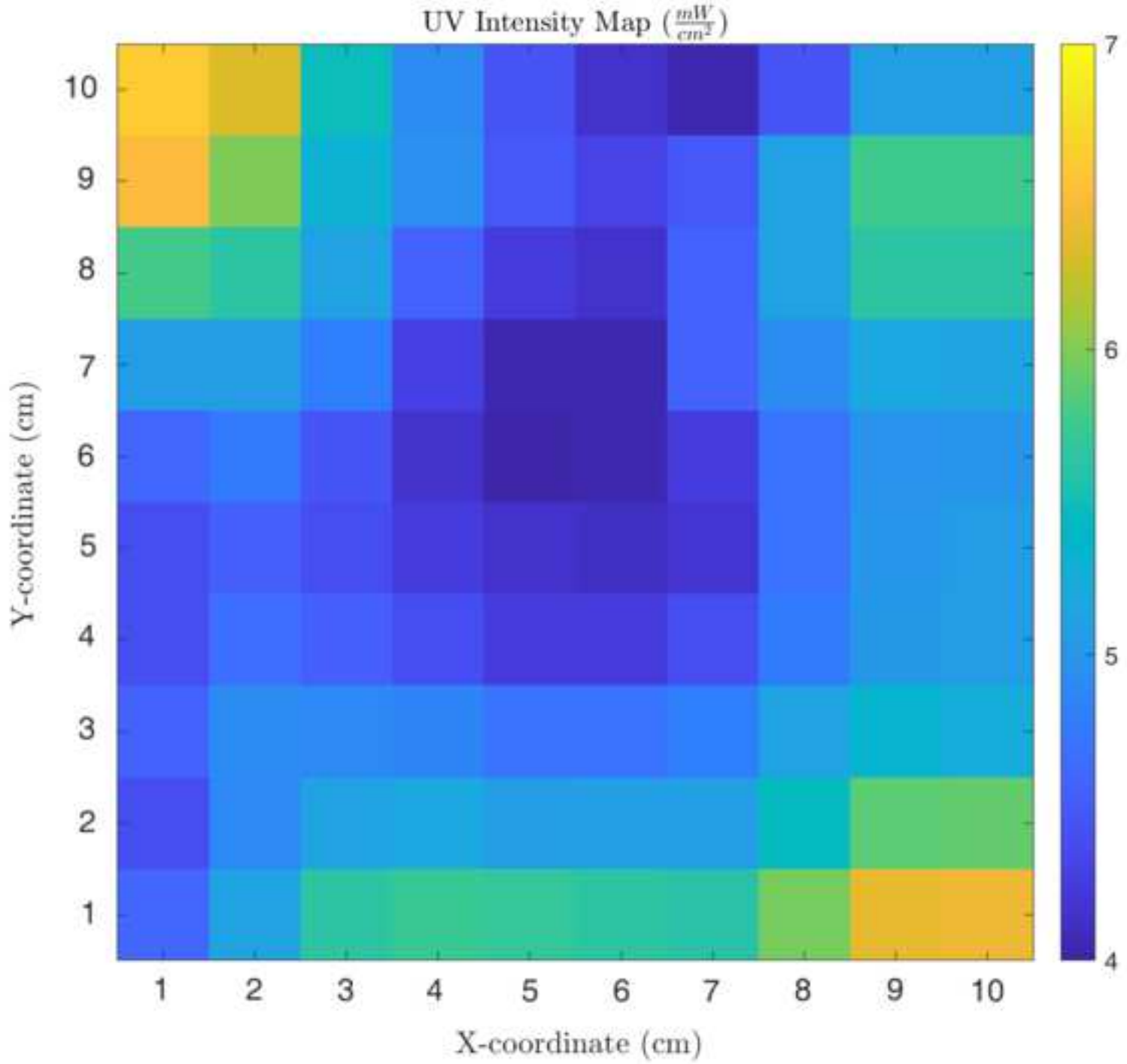

Table of Materials

Name of Material/ Equipment/Software	Company
1/4” bolts and nuts	
3.45 x 3.45 mm UV LED	Kingbright
3D measuring Laser microscope	OLYMPUS
40 mm x 40 mm x 10 mm 12V DC Cooling Fan	Uxcell
120 mm x 38 mm 24V DC Cooling Fan	Uxcell
5 ml (6 ml) NORM-JECT Syringe	HENKE SASS WOLF
Acetone (Certified ACS)	Fisher Chemical
Acid/ corossion resistive tweezer	TED PELLA
Acid/solvent resistance tweezers	TED PELLA, INC
Alloy X	AMERICAN SPECIAL METALS
Ammonium hydroxide (ACS reagent)	Sigma Aldrich
AutoCAD	Autodesk, San Rafael, CA
BD Etchant for PSG-SiO_2 systems	TRANSENE
Blank Borofloat substrate	TELIC
Borofloat substrate with metalizations	TELIC
Capture One photo editing software	Phase One
Capture station	DT Scientific
Carbon dioxide gas (Grade E)	PRAXAIR
Chromium etchant 1020	TRANSENE
Circulating baths with digital temperature controller	PolyScience
CO_2	Airgas
Computer	
Custom made high pressure glass chip holder	
Cutrain (Custom)	
Deionized water (DI)	
Digital camera with monochromatic 60 MP sensor	Phase One
Ethanol, Anhydrous, USP Specs	DECON LABORATORIES, INC.
Facepiece reusable respirator	3M
Fused Silica (UV Grade) wafer	SIEGERT WAFER
GIMP	Open-source image processing software

Glovebox (vinyl anaerobic chamber)	Coy
Heated ultrasonic cleaning bath	Fisher Scientific
Hexamethyldisilazane (HMDS) Cleanroom® MB	KMG
Hose (PEEK tubing)	IDEX HEALTH & SCIENCE
Hydrochloric acid, certified ACS plus	Fisher Chemical
Hydrogen Peroxide	Fisher Chemical
ImageJ	NIH
ISCO syringe pump	TELEDYNE ISCO
Kaiser LED light box	Kaiser
Laser printing machine	LightFab GmbH, Germany.
Laser safety glasses	FreeMascot
LED Engin 5W UV Lens	LEDiL
Light Fab 3D Printer (femtosecond laser)	Light Fab
LightFab 3D printer	LightFab GmbH, Germany
MATLAB	MathWorks, Inc., Natick, MA
Metallic plates	
Micro abrasive sand blasters (Problast 2)	VANIMAN
MICROPOSIT 351 developer	Dow
Muffle furnace	Thermo Scientific
N_2 pure research grade	Airgas
NMP semiconductor grade - 0.1µm Filtered	Ultra Pure Solutions, Inc
Oven	Gravity Convection Oven
Phase One IQ260 with an achromatic sensor	Phase One
Photomask	Fine Line Imaging
Photoresist (SU-8)	MICRO CHEM
Polarized light microscope	OLYMPUS
Ports (NanoPort Assembly)	IDEX HEALTH & SCIENCE
Python	Python Software Foundation
Safety face shield	Sellstrom
Sealing film (Parafilm)	Bemis Company, Inc
Shutter Control Software	Schneider-Kreuznach
Smooth ceramic plates	

Stirring hot plate	Corning®
Sulfuric acid, ACS reagent 95.0-98.0%	Sigma Aldrich
Syringe pump (Standard Infuse/Withdraw PHD ULTRA)	Harvard Apparatus
Torque wrench	Snap-on
UV power meter	Optical Associates, Incorporated
UV power meter	Optical Associates, Incorporated
UV radiation stand (LED lights)	
Vaccum pump	WELCH VACCUM TECHNOLOGY, INC
Variable DC power supplies	Eventek

Catalog Number

LEXT OLS4000

Lot #16M14CB
Lot #177121

#53009 and #53010
Heat Number: ZZ7571XG11
Lot #SHBG9007V

Lot #028934

CG-HF
PG-HF-LRC-Az1500

DT Versa
UN 1013, CAS Number 124-38-9
Lot #025433

100% pure - 001013 - CAS: 124-38-9

NVIDIA Tesla K20 Graphic Card - 706 MHz Core - 5 GB GDDR5 SDRAM - PCI Express 2.0 x16

IQ260
Lot #A12291505J, CAS# 64-17-5
6502QL, Gases, Vapors, Dust, Medium
UV grade

62115
Natural 1/16" OD x .010" ID x 5ft, Part # 1531
Lot # 187244
H325-500

D-SERIES (100DM, 500D)

FILL
B07PPZHNX4

Problast 2 – 80007
10016652
Thermolyne Type 1500
Research Plus - NI RP300
Lot #02191502T
18EG
IQ260
20,320 DPI FILM
Product item: Y0201004000L1PE, Lot Number: 18110975
BX51
NanoPort Assembly Headless, 10-32 Coned, for 1/16" OD, Part # N-333

S32251

PC-620D
Lot # SHBK0108
70-3006
TE25A-34190
Model 308
Model 308

1380
KPS305D

Comments/Description
For fabrication of the metallic plates to sandwich the glass chip between them for thermal bonding
To emitt LED light
To measure channel depths
To cool the UV LED lights
To cool the UV LED lights
To rinse the chip before each experiment
For cleaning
To handle the glass piece in corosive solutions
To handle the glass in corrosive solutions
To clean the chip at the end of process
To design 2D patterns and 3D chips
An improved buffered etch formulation for delineation of phosphosilica glass – SiO_2 (PSG), and borosilica glass – SiO_2 (BSG) systems
Upper substrate for UV etching
Lower substrate for UV etching
To Capture/Edit/Convert the pictures taken by Phase One Camera
To place of the chip in the field of view of the camera
non-aqeous portion of foam
High-purity ceric ammonium nitrate systems for precise, clean etching of chromium and chromium oxide films.
To control the brine and CO_2 temperatures
For CO_2/$scCO_2$ injection
To process and visualize the images obtained via the Phase One camera
To tightly hold the chip and its connections for high pressure testing
To protect against UV/IR Radiations
For cleaning
Visualization system
For cleaning
To protect against volatile solution inhalation
Glass precursor for SLE printing
To characterize image texture and properties

To provide a clean, dust-free environment
To accelerate the etching process
Primer for photoresist coating
Flow connections
Solvent in RCA semiconductor cleaning protocol
Solvent in RCA semiconductor cleaning protocol
To characterize image texture and properties
To pump the fluids
To illuminate the chip
Glass-SLE chip fabrication
To protect against UV/IR Radiations
To emitt LED light
To selectively laser Etch of fused silica
To SLE print the fused silica chips
To characterize image texture and properties

To craete holes in cover plates
Photoresist developer solution
Thermal bonding
For drying the chips in each step
Organic solvent

To visulize transport in microfluidic devices using an ISO 200 setting and an aperture at f/8.
Pattern of channels
Photoresist
Visual examination of micro channels
Connections to the chip
To characterize image texture and properties
To protect against UV/IR Radiations
Isolation of containers
To adjust shutter settings

To heat the solutions
Solvent in RCA semiconductor cleaning protocol
To saturate the chip before each experiment
To tighten the screws
To measure the intesity of UV light
To quantify the strength of UV light
To transfer the pattern to glass (photoresist layer)
To dry the chip
To power the UV LED lights

Thank you for the constructive comments and questions. Please see below for a list of authors' revisions and responses.

1) Confusing sentence – please simplify.

Changed from These limitations have led to a dearth of experimental evidence from direct observation of flow in fractures in microfluidic devices under conditions that are often encountered in the subsurface, i.e., high pressure and temperature conditions

To: As a result, these platforms have not been fully exploited for direct observation of high-pressure transport in fractures.

2) Provide a sample mask as a supplementary.

A picture of a photomask is added to the ESI and a reference to Figures 1 and 1S are added in the text.

3) What tools are used for handling?

The text is revised to include that information:
"Using gloved hands, place the mask …"

4) Mention light wavelength and intensity.

The following information is added under 2.2.2:
"This work uses UV light with a wavelength of 365 nm (to match the peak sensitivity of the photoresist) and at an average intensity of 4.95 mW/cm^2."

5) What tools are used for handling?

The following information in added to the text:
"… using gloved hands".

6) How? How thick is the layer?

The following information is added at the end of the note under 2.5:
"The thickness of this protective layer is immaterial to the overall fabrication process."
Also, the "Using a brush, .." in 2.5.1 addresses the how question.

7) This should be re-written as a step.

2.5.1. Done. Step 2.5.3: "Pour an adequate amount of the etchant into a plastic container and fully submerge the substrate in the etchant."

8) What tools are used for handling?

The following information is added in 2.5.5.: ".. using a solvent-resistant pair of tweezers…"

9) Describe cascade rinse in more detail.

2.3.1. That information is added to step 2.3.3: "Cascade-rinse the substrate by flowing DI water from the top of the substrate and over all its surfaces a minimum of three times and allow the substrate to dry."

10) What magnification and settings?

The relevant information is added to the note under 2.5.6:

NOTE: This characterization may be done using a laser scanning confocal microscope (**Figure 3**). In this work, a x10 magnification is used for data acquisition.

11) Figures must be listed in the order in which they are referenced. Currently Fig 5 is referenced before 3 and 4.

Done.

12) % in 3.1.2

Details of the chemicals are added: "… with acetone (ACS grade), followed by ethanol (ACS grade) …"

13) The editor references a note on "NMP" – we did not find that note. We assume that the editor is asking for more information regarding the heating process.

That information is added in 3.1.1 and 3.1.3: "…. using a hot plate under a hood …"

14) Mention imaging settings including magnification and lens NA

The following information is added: "… using laser scanning confocal microscopy. This work uses a x10 magnification for data acquisition…"

15) Mention all settings.

The following information is added: "… micro abrasive sandblaster and 50-mirometer aluminum-oxide micro sandblasting media."

16) Define.

RCA cleaning is a well-known and well-established procedure; there is a Wikipedia page along with many other sources of information on the topic. See:
https://en.wikipedia.org/wiki/RCA_clean

RCA refers to the place of work of the person who developed the procedure in 1965. We are of the opinion that it should be left as is in the text.

17) Unclear what is done here. Please describe all steps if you wish to film this.

This is a well-known procedure – we have removed it from the list of items to be filmed

18) Should this and the following be substeps of 3.2.4?

Not in our opinion.

19) Unclear which two substrates. Clarify if you mean cover plate and substrate.

Yes. The text has been revised as "Press the substrate and the cover plate…".

20) Provide specifications of these wafers.

The text has been revised to clarify

" … the stacked substrates (the etched substrate and the cover plate) …". In the context of the preceding steps, this change will clarify the intent of the authors.

21) Specifications?
The following information is added: "… two smooth, 1.52 cm-thick, glass-ceramic plates for bonding." The note under step 3.3.3 provides additional details and references a figure that will provide an image of the setup.

22) Molarity?
"… (12.1 mol/L) …" is added to the text.

23) Mention frequency and amplitude.
The following information is added: "… (40 kHz at 100 W of power)…"

24) Provide example
Done. "…(such as lauramidopropyl betaine and alpha-olefin-sulfonate)…"

25) Sentence needs to be check for grammar. Something is not right. Where is it filled? And how? How much volume? Define. Please remember to avoid product names.
Revised as: "Fill the tanks of the CO_2 and water pumps with adequate amount of fluids per the experiment at room temperature."

26) How? And how much?
1.1.1. Revised as: "Fill the brine accumulator and flow lines with the surfactant solution using a syringe. This work uses an accumulator with a capacity of 40 mL."

27) How and when was this done?
1.2. Step 5.1 is added as: "Saturate the microfluidic device with the resident fluid (e.g., DI water, surfactant solution, oil, etc. depending on the type of experiment) using a syringe pump. "

28) Specifications?
Revised as: "…using 0.010" inner diameter tubing…"

29) Please reorder your figures.
Done.

30) Check grammar.
Revised as: "Increase the temperature of the circulating bath, which controls the temperature of the brine and CO_2 lines, to the desired temperature …"

31) Provide all specs.
Revised as: " … This work uses a camera featuring a 60 megapixel, monochromatic, full-frame sensor."

ELSEVIER LICENSE
TERMS AND CONDITIONS

Feb 12, 2020

This Agreement between The University of Kansas -- Hooman Hosseini ("You") and Elsevier ("Elsevier") consists of your license details and the terms and conditions provided by Elsevier and Copyright Clearance Center.

All payments must be made in full to CCC. For payment instructions, please see information listed at the bottom of this form.

License Number	4766641303996
License date	Feb 12, 2020
Licensed Content Publisher	Elsevier
Licensed Content Publication	Current Opinion in Colloid & Interface Science
Licensed Content Title	3D-printed glass microfluidics for fluid dynamics and rheology
Licensed Content Author	Noa Burshtein,San To Chan,Kazumi Toda-Peters,Amy Q. Shen,Simon J. Haward
Licensed Content Date	Oct 1, 2019
Licensed Content Volume	43
Licensed Content Issue	n/a
Licensed Content Pages	14
Start Page	1

End Page	14
Type of Use	reuse in a journal/magazine
Requestor type	academic/educational institute
Portion	figures/tables/illustrations
Number of figures/tables/illustrations	1
Format	electronic
Are you the author of this Elsevier article?	No
Will you be translating?	No
Title of new article	Novel Microfluidic Fabrication Techniques for High-Pressure Testing of Microscale Supercritical CO2 Foam Transport in Fracture/Matrix for Unconventional Oil Recovery
Lead author	Hooman Hosseini
Title of targeted journal	Journal of Visualized Experiments
Publisher	MyJove Corp
Expected publication date	May 2020
Portions	Figure 1
Requestor Location	The University of Kansas Rm. 4132 Learned Hall 1530 W. 15th LAWRENCE, KS 66045 United States Attn: The University of Kansas

Publisher Tax ID	98-0397604
Billing Type	Credit Card
Credit card info	Visa ending in 7236
Credit card expiration	11/2023
Total	32.20 USD

Terms and Conditions

INTRODUCTION

1. The publisher for this copyrighted material is Elsevier. By clicking "accept" in connection with completing this licensing transaction, you agree that the following terms and conditions apply to this transaction (along with the Billing and Payment terms and conditions established by Copyright Clearance Center, Inc. ("CCC"), at the time that you opened your Rightslink account and that are available at any time at http://myaccount.copyright.com).

GENERAL TERMS

2. Elsevier hereby grants you permission to reproduce the aforementioned material subject to the terms and conditions indicated.

3. Acknowledgement: If any part of the material to be used (for example, figures) has appeared in our publication with credit or acknowledgement to another source, permission must also be sought from that source. If such permission is not obtained then that material may not be included in your publication/copies. Suitable acknowledgement to the source must be made, either as a footnote or in a reference list at the end of your publication, as follows:

"Reprinted from Publication title, Vol /edition number, Author(s), Title of article / title of chapter, Pages No., Copyright (Year), with permission from Elsevier [OR APPLICABLE SOCIETY COPYRIGHT OWNER]." Also Lancet special credit - "Reprinted from The Lancet, Vol. number, Author(s), Title of article, Pages No., Copyright (Year), with permission from Elsevier."

4. Reproduction of this material is confined to the purpose and/or media for which permission is hereby given.

5. Altering/Modifying Material: Not Permitted. However figures and illustrations may be altered/adapted minimally to serve your work. Any other abbreviations, additions, deletions and/or any other alterations shall be made only with prior written authorization of Elsevier Ltd. (Please contact Elsevier at permissions@elsevier.com). No modifications can be made to any Lancet figures/tables and they must be reproduced in full.

6. If the permission fee for the requested use of our material is waived in this instance, please be advised that your future requests for Elsevier materials may attract a fee.

7. Reservation of Rights: Publisher reserves all rights not specifically granted in the combination of (i) the license details provided by you and accepted in the course of this licensing transaction, (ii) these terms and conditions and (iii) CCC's Billing and Payment terms and conditions.

8. License Contingent Upon Payment: While you may exercise the rights licensed immediately upon issuance of the license at the end of the licensing process for the transaction, provided that you have disclosed complete and accurate details of your proposed use, no license is finally effective unless and until full payment is received from you (either by publisher or by CCC) as provided in CCC's Billing and Payment terms and conditions. If full payment is not received on a timely basis, then any license preliminarily granted shall be deemed automatically revoked and shall be void as if never granted. Further, in the event that you breach any of these terms and conditions or any of CCC's Billing and Payment terms and conditions, the license is automatically revoked and shall be void as if never granted. Use of materials as described in a revoked license, as well as any use of the materials beyond the scope of an unrevoked license, may constitute copyright infringement and publisher reserves the right to take any and all action to protect its copyright in the materials.

9. Warranties: Publisher makes no representations or warranties with respect to the licensed material.

10. Indemnity: You hereby indemnify and agree to hold harmless publisher and CCC, and their respective officers, directors, employees and agents, from and against any and all claims arising out of your use of the licensed material other than as specifically authorized pursuant to this license.

11. No Transfer of License: This license is personal to you and may not be sublicensed, assigned, or transferred by you to any other person without publisher's written permission.

12. No Amendment Except in Writing: This license may not be amended except in a writing signed by both parties (or, in the case of publisher, by CCC on publisher's behalf).

13. Objection to Contrary Terms: Publisher hereby objects to any terms contained in any purchase order, acknowledgment, check endorsement or other writing prepared by you, which terms are inconsistent with these terms and conditions or CCC's Billing and Payment terms and conditions. These terms and conditions, together with CCC's Billing and Payment terms and conditions (which are incorporated herein), comprise the entire agreement between you and publisher (and CCC) concerning this licensing transaction. In the event of any conflict between your obligations established by these terms and conditions and those established by CCC's Billing and Payment terms and conditions, these terms and conditions shall control.

14. Revocation: Elsevier or Copyright Clearance Center may deny the permissions described in this License at their sole discretion, for any reason or no reason, with a full refund payable to you. Notice of such denial will be made using the contact information provided by you. Failure to receive such notice will not alter or invalidate the denial. In no event will Elsevier or Copyright Clearance Center be responsible or liable for any costs, expenses or damage incurred by you as a result of a denial of your permission request, other than a refund of the amount(s) paid by you to Elsevier and/or Copyright Clearance Center for denied permissions.

LIMITED LICENSE

The following terms and conditions apply only to specific license types:

15. **Translation**: This permission is granted for non-exclusive world **English** rights only unless your license was granted for translation rights. If you licensed translation rights you may only translate this content into the languages you requested. A professional translator must perform all translations and reproduce the content word for word preserving the integrity of the article.

16. **Posting licensed content on any Website**: The following terms and conditions apply as follows: Licensing material from an Elsevier journal: All content posted to the web site must maintain the copyright information line on the bottom of each image; A hyper-text must be included to the Homepage of the journal from which you are licensing at http://www.sciencedirect.com/science/journal/xxxxx or the Elsevier homepage for books at http://www.elsevier.com; Central Storage: This license does not include permission for a scanned version of the material to be stored in a central repository such as that provided by Heron/XanEdu.

Licensing material from an Elsevier book: A hyper-text link must be included to the Elsevier homepage at http://www.elsevier.com . All content posted to the web site must maintain the copyright information line on the bottom of each image.

Posting licensed content on Electronic reserve: In addition to the above the following clauses are applicable: The web site must be password-protected and made available only to bona fide students registered on a relevant course. This permission is granted for 1 year only. You may obtain a new license for future website posting.

17. **For journal authors:** the following clauses are applicable in addition to the above:

Preprints:

A preprint is an author's own write-up of research results and analysis, it has not been peer-reviewed, nor has it had any other value added to it by a publisher (such as formatting, copyright, technical enhancement etc.).

Authors can share their preprints anywhere at any time. Preprints should not be added to or enhanced in any way in order to appear more like, or to substitute for, the final versions of articles however authors can update their preprints on arXiv or RePEc with their Accepted Author Manuscript (see below).

If accepted for publication, we encourage authors to link from the preprint to their formal publication via its DOI. Millions of researchers have access to the formal publications on ScienceDirect, and so links will help users to find, access, cite and use the best available version. Please note that Cell Press, The Lancet and some society-owned have different preprint policies. Information on these policies is available on the journal homepage.

Accepted Author Manuscripts: An accepted author manuscript is the manuscript of an article that has been accepted for publication and which typically includes author-incorporated changes suggested during submission, peer review and editor-author communications.

Authors can share their accepted author manuscript:

- immediately
    - via their non-commercial person homepage or blog
    - by updating a preprint in arXiv or RePEc with the accepted manuscript
    - via their research institute or institutional repository for internal institutional uses or as part of an invitation-only research collaboration work-group
    - directly by providing copies to their students or to research collaborators for their personal use
    - for private scholarly sharing as part of an invitation-only work group on commercial sites with which Elsevier has an agreement
- After the embargo period
    - via non-commercial hosting platforms such as their institutional repository
    - via commercial sites with which Elsevier has an agreement

In all cases accepted manuscripts should:

- link to the formal publication via its DOI
- bear a CC-BY-NC-ND license - this is easy to do
- if aggregated with other manuscripts, for example in a repository or other site, be shared in alignment with our hosting policy not be added to or enhanced in any way to appear more like, or to substitute for, the published journal article.

Published journal article (JPA): A published journal article (PJA) is the definitive final record of published research that appears or will appear in the journal and embodies all value-adding publishing activities including peer review co-ordination, copy-editing, formatting, (if relevant) pagination and online enrichment.

Policies for sharing publishing journal articles differ for subscription and gold open access articles:

Subscription Articles: If you are an author, please share a link to your article rather than the full-text. Millions of researchers have access to the formal publications on ScienceDirect, and so links will help your users to find, access, cite, and use the best available version.

Theses and dissertations which contain embedded PJAs as part of the formal submission can be posted publicly by the awarding institution with DOI links back to the formal publications on ScienceDirect.

If you are affiliated with a library that subscribes to ScienceDirect you have additional private sharing rights for others' research accessed under that agreement. This includes use for classroom teaching and internal training at the institution (including use in course packs and courseware programs), and inclusion of the article for grant funding purposes.

Gold Open Access Articles: May be shared according to the author-selected end-user license and should contain a CrossMark logo, the end user license, and a DOI link to the formal publication on ScienceDirect.

Please refer to Elsevier's posting policy for further information.

18. **For book authors** the following clauses are applicable in addition to the above: Authors are permitted to place a brief summary of their work online only. You are not allowed to download and post the published electronic version of your chapter, nor may you scan the printed edition to create an electronic version. **Posting to a repository:** Authors are permitted to post a summary of their chapter only in their institution's repository.

19. **Thesis/Dissertation**: If your license is for use in a thesis/dissertation your thesis may be submitted to your institution in either print or electronic form. Should your thesis be published commercially, please reapply for permission. These requirements include permission for the Library and Archives of Canada to supply single copies, on demand, of the complete thesis and include permission for Proquest/UMI to supply single copies, on demand, of the complete thesis. Should your thesis be published commercially, please reapply for permission. Theses and dissertations which contain embedded PJAs as part of the formal submission can be posted publicly by the awarding institution with DOI links back to the formal publications on ScienceDirect.

Elsevier Open Access Terms and Conditions

You can publish open access with Elsevier in hundreds of open access journals or in nearly 2000 established subscription journals that support open access publishing. Permitted third party re-use of these open access articles is defined by the author's choice of Creative Commons user license. See our open access license policy for more information.

Terms & Conditions applicable to all Open Access articles published with Elsevier:

Any reuse of the article must not represent the author as endorsing the adaptation of the article nor should the article be modified in such a way as to damage the author's honour or reputation. If any changes have been made, such changes must be clearly indicated.

The author(s) must be appropriately credited and we ask that you include the end user license and a DOI link to the formal publication on ScienceDirect.

If any part of the material to be used (for example, figures) has appeared in our publication with credit or acknowledgement to another source it is the responsibility of the user to ensure their reuse complies with the terms and conditions determined by the rights holder.

Additional Terms & Conditions applicable to each Creative Commons user license:

CC BY: The CC-BY license allows users to copy, to create extracts, abstracts and new works from the Article, to alter and revise the Article and to make commercial use of the Article (including reuse and/or resale of the Article by commercial entities), provided the user gives appropriate credit (with a link to the formal publication through the relevant DOI), provides a link to the license, indicates if changes were made and the licensor is not represented as endorsing the use made of the work. The full details of the license are available at http://creativecommons.org/licenses/by/4.0.

CC BY NC SA: The CC BY-NC-SA license allows users to copy, to create extracts, abstracts and new works from the Article, to alter and revise the Article, provided this is not done for commercial purposes, and that the user gives appropriate credit (with a link to the formal publication through the relevant DOI), provides a link to the license, indicates if changes were made and the licensor is not represented as endorsing the use made of the work. Further, any new works must be made available on the same conditions. The full details of the license are available at http://creativecommons.org/licenses/by-nc-sa/4.0.

CC BY NC ND: The CC BY-NC-ND license allows users to copy and distribute the Article, provided this is not done for commercial purposes and further does not permit distribution of the Article if it is changed or edited in any way, and provided the user gives appropriate credit (with a link to the formal publication through the relevant DOI), provides a link to the license, and that the licensor is not represented as endorsing the use made of the work. The

full details of the license are available at http://creativecommons.org/licenses/by-nc-nd/4.0. Any commercial reuse of Open Access articles published with a CC BY NC SA or CC BY NC ND license requires permission from Elsevier and will be subject to a fee.

Commercial reuse includes:

- Associating advertising with the full text of the Article
- Charging fees for document delivery or access
- Article aggregation
- Systematic distribution via e-mail lists or share buttons

Posting or linking by commercial companies for use by customers of those companies.

20. **Other Conditions**:

v1.9

Questions? customercare@copyright.com or +1-855-239-3415 (toll free in the US) or +1-978-646-2777.

Electronic Supplementary Information

Microfluidic Fabrication Techniques for High-Pressure Testing of Microscale Supercritical CO_2 Foam Transport in Fractured Unconventional Reservoirs

Hooman Hosseini, Feng Guo, Reza Barati Ghahfarokhi, Saman A. Aryana

Correspondence to: Saman A. Aryana, Reza Barati Ghahfarokhi
E-mail: saryana@uwyo.edu, reza.barati@ku.edu

This PDF file includes:

Figure S1, S2, S3, S4 and S5

1- Photolithography and thermal bonding for borosilicate glass substrates

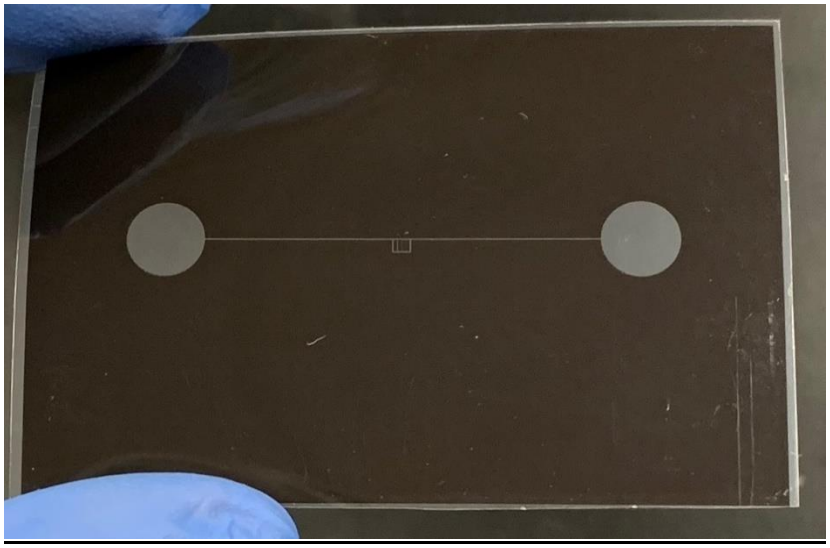

Figure S1. Photomask.

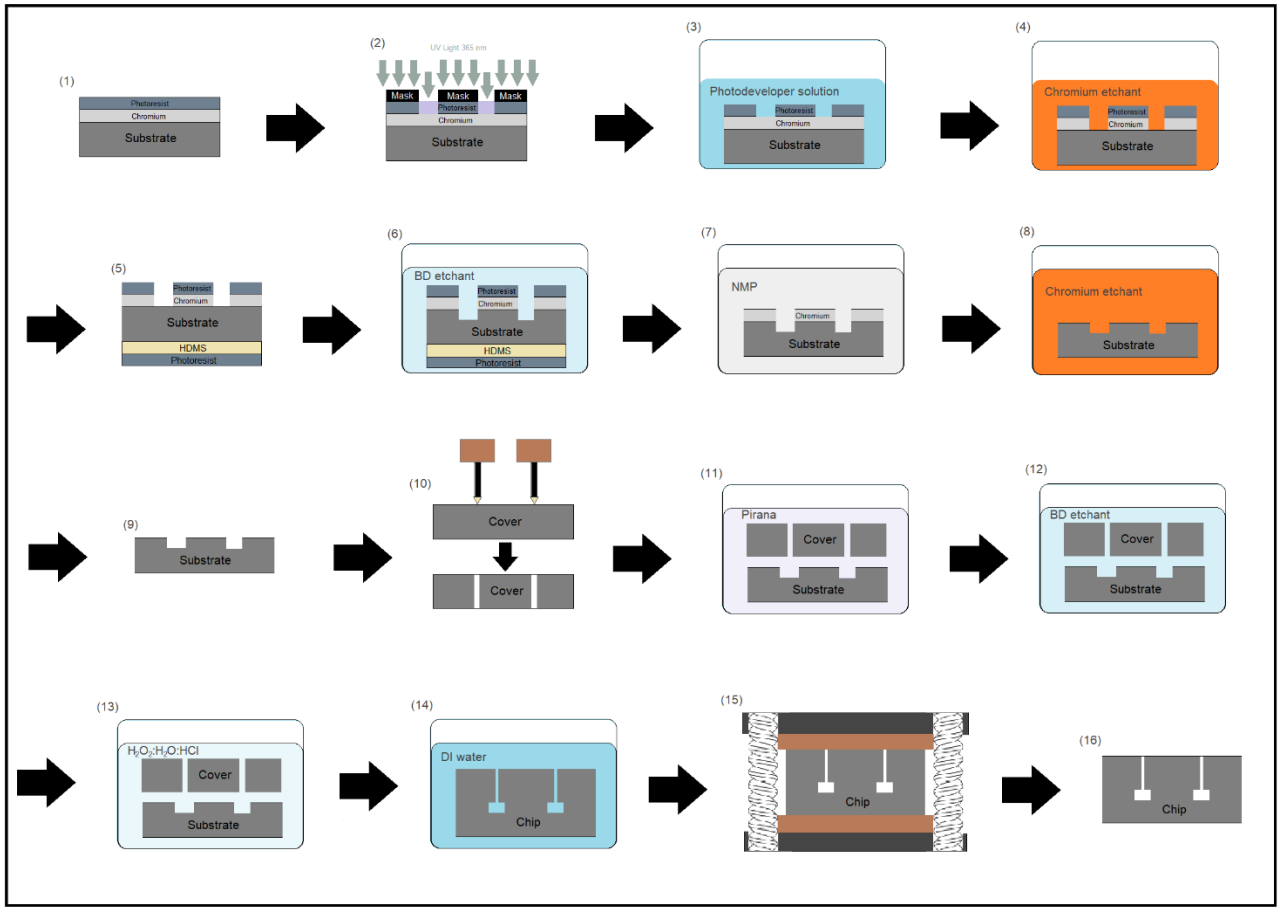

Figure S2. Schematic of the photolithography and thermal bonding fabrication process.

Figure S1 shows an example of a photomask designed for a positive photoresist. This mask is used to transfer the desired pattern onto a borosilicate glass. Figure S2 illustrates the schematic of the photolithography and thermal bonding fabrication process in 16 steps (for brevity, cascade-rinsing of the substrates with DI water is excluded): 1) obtaining borosilicate glass substrate coated with chromium and photoresist layers; 2) UV- radiation on the substrate for a pre-determined amount of time to transfer the pattern from the photomask to the photoresist layer; 3) using a developer solution to dissolve the radiated features in the positive photoresist; 4) submerging the substrate in chromium etchant (40°C) for 40 s to transfer the pattern from the photoresist to the chrome layer; 5) coating the backside of the borosilicate glass with HMDS and photoresist for protection against the etchant; 6) submerging the substrate in the etchant solution for a predetermined amount of time to etch channels with the required depth in the substrate; 7) submerging the etched substrate in NMP (organic solvent) heated to 65°C for 30 min to remove all photoresist; 8) submerging the substrate in chromium etchant heated to 40°C for 40 s to remove the remainder of the chrome layer from the substrate; 9) drying and preparing the fully etched substrate for bonding; 10) sandblasting the cover plate to create inlet/outlets holes; 11) submerging the substrate and the cover-plate in a boiling Piranha solution for 20 min to remove all contaminants; 12) submerging the substrate and the cover-plate in the etchant solution for 30 s to create clean surfaces for bonding; 13) submerging the substrate and the cover plate in a 6:1:1 by volume solution of H_2O: H_2O_2:HCl for 10 min to remove the remaining inorganic impurities; 14) submerging the substrate and the cover plate in

DI water and pressing the matching sides of the two substrates firmly against each other to create a stack for the bonding process; 15) placing the stack between two ceramic and metallic plates and placing the stack in a vacuum oven (70 – 90 °C) for 30 min followed by placing the stack in a furnace and executing the thermal bonding protocol; and 16) the thermally bonded device is ready for testing.

2- In-house developed collimated UV light source

Figure S3 shows an image of in-house collimated UV light source. The LEDs emitters are mounted on a heat sink plate in a 3 × 3 square array with a pitch of 50 mm. The divergence (viewing angle) of light coming from individual LEDs are reduced from ~70° to ~12° by using a commercial light-collecting UV lens to each LED – see Figure S4. To further reduce the divergence (~5°), a 3 × 3 square array (with the same pitch of 50 mm) of nine converging polyvinylchloride (PVC) Fresnel lenses with a focal length f ≈ 180 mm are used. These lenses are mounted on a black acrylic plate. The distance between the acrylic plate and LED lights is adjustable. In order to achieve an even illumination (function of the current), three separate adjustable power supplies (30 v, 5 A) are employed to power the LED array. To adjust the illumination, the currents through the four LEDs in the corners, four LEDs at the edges, and the LED in the center are regulated separately by different power supplies.

A schematic of the optical setup of the LED UV light source is illustrated by Figure S4. Given the relatively large distance between the individual LEDs and the low beam divergence, the light source in the setup is placed at a sufficient distance from the target to achieve sufficient beam overlap, which results to a uniform illumination; the distance from the LED plate to the substrate holder is 960 mm. The mounting setup includes aluminum extrusions, connecting plates and brackets, from 80/20. The design helps to align the light source with the substrate holder and adjust the distance between the Fresnel lens array and the LED array for optimal illumination.

Figure S3. Image of UV LED lights source

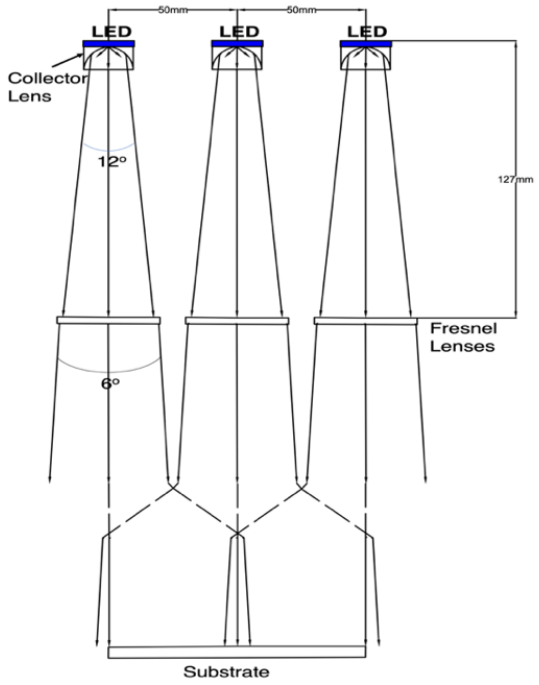

Figure S4. Schematic of the LED UV-light source

The relative uniformity of this collimated UV light source improves the consistency of microfluidic device fabrication and reduces the deviation between fabricated pore network and designed pore network. The narrow spectrum of the LEDs, which is centered at ~365 nm, corresponding to an SU-8 2000 absorption wave length of 350-400 nm, leads to a relatively weak dependence of the optimal exposure time on the thickness of photoresist layer, which makes the fabrication process more forgiving. The exposure areas illuminated by individual LEDs provide UV illumination with a mean intensity of ~4.95 mW cm^{-2} over a 100 × 100 mm^2 target area. In this work, a single exposure time of 2 min is used, which corresponds to a cumulative irradiation of ~240 mJ cm^{-2}. This collimated UV light source enables fabrication of microfluidic devices with consistent and accurate channel networks.

3- High-pressure holders for the microfluidic device

Figure S5 shows a close-up view of high-pressure holders The holder comprises two piece made of 304 stainless steel. As shown in FigureS5, these plates feature an opening that accommodates the typical microfluidic devices built in the laboratory at the University of Wyoming. The two plates are connected via hex socket cap screws. Inlet-outlet lines are fixed in place via the threaded through-hole in each holder, which protects the ports from leaks mechanically by applying compressive force against the sandblasted hole in the device. As such, the holders also protect the microfluidic device from dislocation during high pressure injection without the need for adhesive-based sealants. The through-hole in the holder and the hex socket cap screws are shown in Figure S4. The hex socket cap screws are spaced center-to-center 35 mm apart. The top plate (Figure S5) is 43 mm x 150 mm x 12 mm thick, and the bottom plate is 43 mm x 150 mm x 5 mm thick. The housing for the microfluidic device is 112

mm x 25 mm deep x 5 mm high; it is formed in the top plate and reduces the thickness of the top plate to 7 mm.

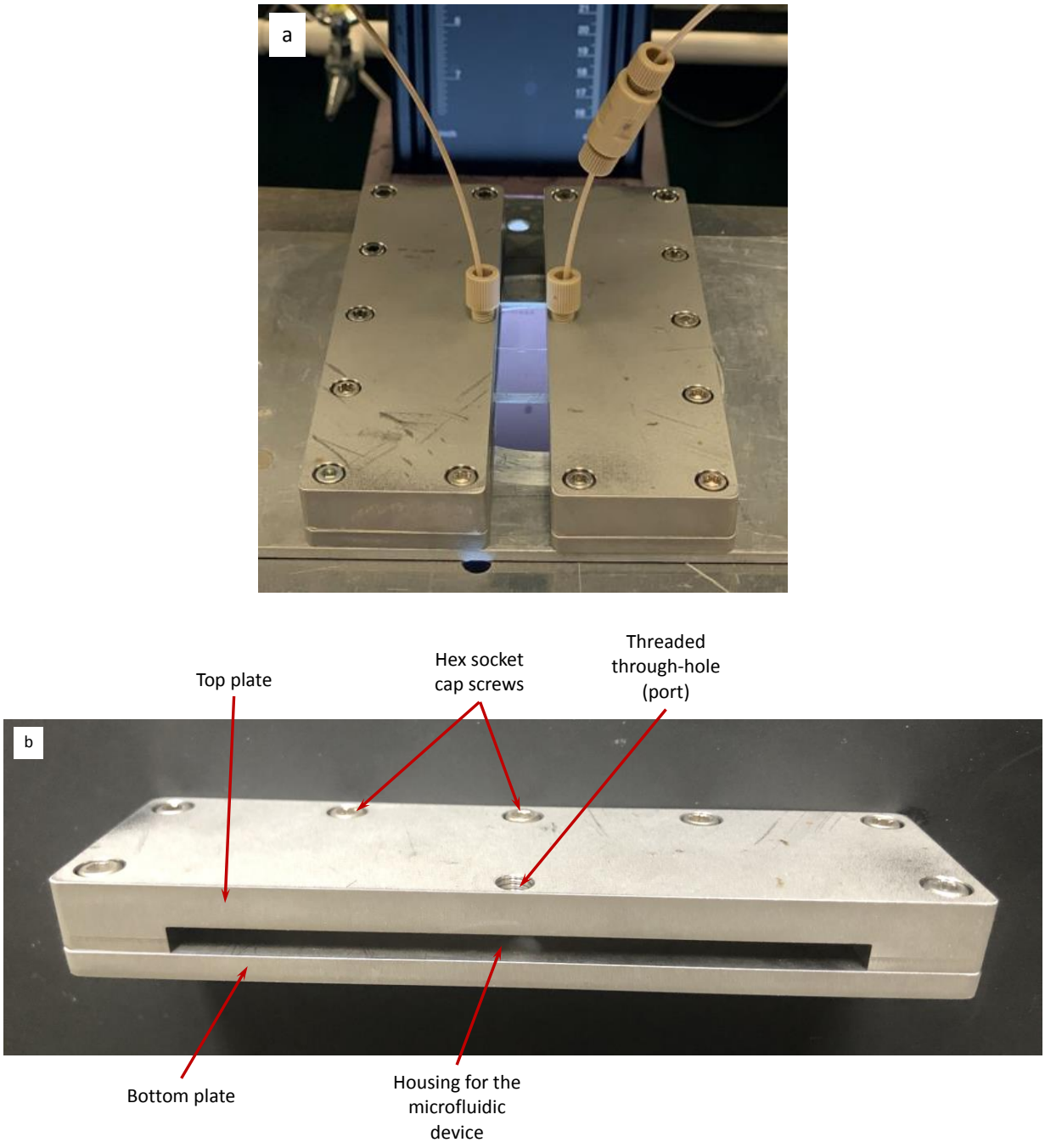

Figure S5. High-pressure holder for microfluidic devices; a) close-up view of the holders during a flow experiment, and b) close-up view of a single holder.